VARIATION IN WING AREA AND PREY DETECTION VOLUME OF *RHINOLOPHUS CAPENSIS* IN RESPONSE TO DIFFERENT CLIMATES

Aurora Duncan

Dissertation presented for the degree Master of Science in the Department of Biological Sciences

at the University of Cape Town

August 2020

Supervisor: David Jacobs

TABLE OF CONTENTS

DECLARATION

I know the meaning of plagiarism and declare that all of the work in this thesis, save for that which is properly acknowledged, is my own.

Signature: Signed by candidate Date: 30 August 2020

Dedication

I would like to dedicate this thesis to the Duncan and De Vos families. First, my mom, dad, and brother, who despite being halfway across the world, managed to support and encourage me in every way they could. Second, thank you to my Cape Town family: Marc, Lauren, Marilyn, and Eon. I cannot thank you all enough for the support you have provided me.

ACKNOWLEDGEMENTS

I would like to first thank my supervisor, Prof. David Jacobs, for his expertise during this process. His vast knowledge on bats and the research process have been an invaluable resource to me. I am very grateful for the interesting conversations and detailed feedback on my work. Thank you for always encouraging me to explore different facets of knowledge and motivating me to aim high.

Next, I would like to thank my lab mates and field assistants for your help in collecting data. My lab mates, David Wechuli and Victor Mutavhatsindi, were very helpful in explaining the appropriate techniques and being adaptable to ever-changing field conditions. Our field assistants, Tinyiko, Beatrice, Justin, Caton, and Samantha were fantastic people to work with. Their positive attitudes and resilience made them amazing people to have in the field. I would not have been able to collect all the data I needed if not for them. Thank you.

Thank you to Prof. Marc Holderied at Bristol University for guidance in building the multiple microphone array system and for permission to use his MATLAB scripts for the reconstruction of bat flight passes from their echolocation pulses. Thank you to Nikita Finger for permission to use her spreadsheet to calculate the detection distances of echolocation pulses.

Next, thank you to the staff at the various sites I had the pleasure of visiting. First, thank you to the staff at Richtersveld Transfrontier National Park, including park manager Brent Whittington, Nkabeng Mzileni, and Ernest Daemane. Special thanks to Mr. Whittington, who gave fantastic advice on sites to visit and was available at all hours to help. Thank you to the staff at Baviaanskloof Nature Reserve, and especially to Noel Isaacs, who ensured our safety and comfort during our entire stay. Next, thank you to the staff at Sleepy Hollow accommodation in the Eastern Cape. They provided fantastic accommodation and wonderful company during our stay. Being able to access caves on private land is not something to take for granted in the research world, and I thank Anton and his wonderful family for being so enthusiastic when assisting in our research. Finally, thank you to the SanParks rangers at Garden Route National Park. Their field expertise and company is much appreciated.

Next, thank you to Dr. Ben Smit at Rhodes University. I am immensely grateful for your insight and assistance in sampling at the Table Farm site. Dr. Smit helped us at a moment's notice and provided useful advice in the best ways to gather the data we needed. I hope that our lab groups are able to collaborate more in the future.

Finally, a big thank you to the University of Cape Town, especially the Biological Sciences Department, for making my transition to Cape Town easy and enjoyable. This study was funded by grants awarded to Prof. David Jacobs through the National Research Foundation (NRF) and University Research Committee (URC). It was also funded through an NRF Innovation M & D scholarship.

LIST OF TABLES

LIST OF FIGURES

Abstract

Wing shape and echolocation are two novel adaptations in the Chiroptera and are strongly influenced by environmental conditions. Wing shape is influenced by environmental clutter. Shorter, broader wings allow for more maneuverable flight, and are advantageous for bats living in highly cluttered environments. Longer, narrower wings help bats to increase flight speed, and are best suited for bats living in more open environments. It is likely that wing shape is also influenced by temperature, given the potential for wings to act as thermoregulatory appendages. Wings provide a thermal gradient across their surfaces, dissipating excess heat from the body. However, the importance in thermoregulation in determining wing size is unknown. If thermoregulation is a strong selective pressure, bats in hotter, more arid regions should have larger wings.

Environmental conditions also influence echolocation pulse design. Echolocation pulses must successfully reach a target and generate an audible echo despite atmospheric attenuation. High-duty cycle (HDC) pulses, calls with longer durations than the interval between them, are particularly useful in environments with high amount of environmental clutter. HDC echolocators use an acoustic fovea and Doppler shift compensation to detect the fluttering wings of insect prey in dense vegetation. However, the flexibility of these pulses is limited by the bat's acoustic fovea.

Wing shape and echolocation combined form an adaptive complex, providing bats with a highly specialized system of foraging. Climate change poses an enormous risk to a bat's foraging success, because rising ambient temperatures are likely to change the selective pressures on wing size (due to the potential thermoregulatory benefits) as well as prey detection volumes of the bat's echolocation (because sound propagation is influenced by temperature). As an adaptive

complex any selection on either wings or echolocation is likely to influence changes in the other, with consequences for the foraging efficiency of bats. The potential impact of climate change on the foraging efficiency of bats can be gauged by the bats' adaptive responses to different climatic conditions over their geographic range.

I examined these two traits in different localities across the geographic range of the Cape horseshoe bat, *R. capensis* to determine if wing and echolocation parameters are adapted to current climatic conditions. I measured wing area and echolocation parameters at sites within the distribution of *R. capensis* that were representative of the different climates across its range. I measured wing areas using digital image analysis software, and I measured echolocation parameters using a microphone array system. Temperature was a predictor in the top fitting linear mixed effects models for both wing area and prey detection volume. For differences in wing area, body mass was the only significant explanatory variable. However, body mass may itself be influenced by environmental conditions. NDVI, latitude, and average winter minimum temperature significantly related to differences in prey detection volume.

My results indicate geographic variation in both wing area and prey detection volume, an indication that these traits are adapted to local climate conditions. Geographic variation in wing area is a consequence of body mass, which may or may not be a function of climate. However, geographic variation in prey detection volume is directly influenced by the environment. Therefore, increases in ambient temperature due to human-induced climate change are likely to have an effect on the foraging efficiency of *R. capensis*.

Key words: Evolution, ERA5, sensory traits

Introduction

Bats are among the most successful groups of mammals, inhabiting every continent except Antarctica. Most notably, their ability to fly and echolocate have allowed diversification in their morphology, behavior, and diet (Denzinger and Schnitzler, 2013; Norberg and Rayner, 1987). The wide range of traits that exist across bat lineages provide evidence for the acute specialization of these traits to their respective environments. These traits have allowed many insectivorous bat species to become efficient foragers, with some species consuming up to a 84% of their body masses in one evening (Kalka and Kalko, 2006). Evidence has suggested that the abilities of flight and echolocation have formed an "adaptive complex," whereby each of these abilities is strongly influenced by the other (Aldridge and Rautenbach, 1987; Jacobs and Bastian, 2018; Norberg and Rayner, 1987). It is therefore likely that any environmental changes will affect both of these adaptations concurrently across a population.

One of the most serious environmental risks to bats is human-induced climate change. It is projected that climate change could increase Earth's mean temperature between two and four degrees Celsius by the end of the century if proper measures are not taken (IPCC, 2018). Such drastic increases in temperature will force bats to adapt to new environmental conditions, move to a more suitable environment, or face extinction. Environmental changes, including increases in ambient air temperature and more extreme weather events, already pose direct threats to many bats because they are dependent on weather conditions for foraging, reproduction, and roosting (Adams, 2010; Erickson and West, 2002; Sherwin et al., 2013). Bats are more likely to exit their roosts to forage when temperatures within their optimal temperature range (Anthony et al., 1981; Avery, 1985; Klüg-Baerwald et al., 2016). Temperature has also been shown to affect the expression of torpor in species including *Miniopterus schreibersii blepotis* and *Mops condylurus*

(Hall, 1982; Vivier and Van der Merwe, 2007). If bats are more likely to arouse from torpor to forage in higher ambient temperature, it could lead to higher energy expenditure. Reproductive cycles in many temperate-zone bats are also temperature-dependent and closely associated with increases in food availability after winter hibernation (Krishna and Bhatnagar, 2011; Mead, 1993; Racey, 1973, 1969). Increases in ambient temperature leading to earlier parturition have been observed in various species of bats, including *Myotis daubentonii* and *Myotis myotis* (Ibáñez, 1997; Lučan et al., 2013). Such changes in reproductive cycles could be particularly disruptive and lead to reproductive declines (Adams, 2010). Finally, microclimates within roosts are particularly important in determining bat activity, community structure, and successful reproduction. Different species, depending on their thermoregulatory needs, occupy different parts of the same cave (Avila-Flores and Medellín, 2004). Kerth et al. (2001) also found that females will typically select cooler roosts prior to giving birth, and warmer roosts after giving birth. Changes in the ambient temperature within roosts and in foraging areas may decrease the reproductive success of bats, increase the thermoregulatory costs of foraging, and limit the activity time dedicated to finding food. Indirectly, increases in temperature may put bats at a higher risk of catching various diseases, including White Nose Syndrome (Flory et al., 2012; Maher et al., 2012). Extreme weather events, decreases in water availability and overall landscape change also pose a threat to bats (Jones et al., 2009; Sherwin et al., 2013). The ecosystem services that bats provide, including pest control and seed dispersal, make the potential effects of climate change on bats particularly concerning (Sherwin et al., 2013). For example, *Tadarida brasiliensis* accounts for up for USD 741,000 in central pest control in only eight counties in Texas, USA every year (Cleveland et al., 2006). On a global scale, decreases in bat populations would have a significant economic and ecological impact on humans (Sherwin et al., 2013).

Bats have the ability to act as bioindicators, meaning that changes in their populations or activity levels can indicate the overall health of an ecosystem (Jones et al., 2009). Studies have shown bats responding to environmental changes, including ambient air temperature, water quality, and heavy metal pollution (O'Shea and Johnston, 2017; Racey, 1973; Vaughan et al., 1996). Given the potential for bats to act as bioindicators, it is necessary to understand their current adaptations to local climactic conditions (Jones et al., 2009). As the success of most bats hinges on their abilities of flight and echolocation, studying the intraspecific variation of these traits across climates with varying conditions, such as ambient temperature and vegetation cover, is particularly important. Variation in echolocation detection volume and wing size across different climates can provide an indication of how bats may be impacted by climate change.

The adaptability of the structure of the wings has influenced their in-flight maneuverability, agility, and speed, depending on the environmental conditions (Norberg and Rayner, 1987; Vaughan, 1966). For example, a bat's wings must allow maneuverable flight to allow it to navigate around environmental "clutter" (echoes from non-target objects), which includes buildings, plants, trees, or shrubs, while also optimizing its flight speed and maneuverability to successfully catch prey (Falk et al., 2014; Warnecke et al., 2015). Maneuverability depends on both the body mass of the bat and its relative wing size and shape. Maneuverability is an index based on wing loading, which is an index calculated by dividing body weight (body mass x 9.81) by wing area (Norberg and Rayner, 1987). Relative to their body size, bats with short, broad wings typically forage in more cluttered environments (Aldridge and Rautenbach, 1987; Norberg and Rayner, 1987) This wing shape lowers their flight speed, but increases their maneuverability, allowing it to effectively avoid clutter. In contrast, a bat with long, thin wings can fly faster, but is less maneuverable (Fenton, 1990; Norberg and Rayner, 1987). Bats with these wing shapes typically live in environments with more open spaces, where speed and agility are important factors in finding and catching prey (Norberg and Rayner, 1987). Bats with a larger body mass relative to their wing areas are heavier and therefore less maneuverable (Norberg and Rayner, 1987). These bats typically live in less cluttered environments. Contrastingly, bats with a lighter body mass relative to their wing areas are more maneuverable, and forage in more cluttered environments (Aldridge and Rautenbach, 1987; Norberg and Rayner, 1987)

The role of environmental clutter in shaping the size and shape of bat wings has been well-studied across many species (Norberg and Rayner, 1987). Fewer studies have explored the potential selective pressure of thermoregulation on the structure of bat wings, despite the evidence of wings as thermoregulatory tools. Bat wings can assist bats in stabilizing their body temperatures in both hypothermic and hyperthermic conditions. For example, Bartholomew et al. (1964) showed evidence of *Pteropus poliocephalus and Pteropus scapulatus* wrapping their wings around their bodies to create a pocket of air between the wings and bodies which was up to 10 degrees warmer than the ambient air temperature. (Bartholomew et al., 1964; Kluger and Heath, 1970; Reeder and Cowles, 1951). In colder environments, blood flow to their wings is reduced to conserve body heat (Kluger and Heath, 1970; Reeder and Cowles, 1951). When active in high temperatures, bats will pant, lick their bodies, and extend and fan their wings to dissipate heat (Reeder and Cowles, 1951; Vaughan, 1987). At extremely high temperatures, the wing capillaries will widen and fill with blood, allowing heat to radiate from the wings into the surrounding environment more quickly (Widmer et al., 2007). Since caves may act as a temperature stabilizer, it is important for bats to also have thermoregulatory control while foraging (Twente, 1955). The large, flat surface area of the wings creates a thermal gradient between the bat's wings and the surrounding environment, allowing bat wings to dissipate twice as much heat as the body (Lancaster et al., 1997). This thermal gradient has also been observed in *Carollia perspicillata*, with higher heats in the proximal wing than the distal wing (Rummel et al., 2019). Similarly, heat loss through the wings while in flight was observed in an insectivorous bat, *Tadarida brasiliensis,* with much of this excess heat lost through radiative heat loss to the cool night sky (Reichard et al., 2010). This suggests that bats with a larger surface area (i.e. larger wings) may be more successful at dissipating excess heat.

If morphological adaptations act as the primary source of thermoregulation in bats, it is reasonable to suggest that selection would favor larger wings relative to body size in hotter environments. This is especially true of bats in flight, since caves offer a buffer to maintain a more stable body temperature (Kunz and Fenton, 2003; Twente, 1955). Studies on wings as thermoregulatory tools are critical for determining what role wing size may serve in a changing climate. Furthermore, the relationship between wing shape, thermoregulation, and maneuverability must be explored. For example, if larger wings, relative to body size, are favored in hotter environments for effective thermoregulation, are the body masses of the bats also greater to accommodate changes in wing loading? If thermoregulatory use is the stronger selective pressure, one should expect to see larger wing areas in hotter environments where body size is relatively constant. If maneuverability is a stronger selective pressure, than one should expect to see wing loading values that match the degree of environmental clutter.

Along with flight, bats evolved echolocation which allowed them to orientate, navigate, communicate, and hunt prey in complete darkness (Griffin, 1958; Jones and Siemers, 2011;

Knörnschild et al., 2012). Bats emit ultrasonic sounds/pulses from their nostrils or mouths. The pulse is reflected off prey or objects as echoes. These echoes are detected by the bat's ears and interpreted by the auditory cortex of the bat's brain to form a 3-D image of the world around it (Griffin, 1958). As with bat wings, the echolocation pulses employed by bats are varied. Bats use echolocation pulses with different time-frequency structure, frequencies, and durations that are suited to the acoustic properties of the different habitats that bats occupy (Fenton, 1990; Neuweiler et al., 1987).

Different bat lineages have employed different strategies to increase echolocation efficacy in the different habitats in which they echolocate. Bat species that use the larynx to emit sound will use either high-duty cycle (HDC) or low-duty cycle (LDC) echolocation strategies, where the duty cycle is defined as ratio of the duration of the echolocation pulse to its period (Fenton, 1999). Period is the time between the onset of successive pulses (Fenton, 1999). Duty cycle is usually expressed as a percentage (Lazure and Fenton, 2011). These different echolocation strategies are employed to help bats to avoid self-deafening from the high intensity pulses they emit (Rydell, 1995). LDC pulses are comprised of short, frequency-modulated sweeps that vary in bandwidth, duration, and modulation, and are separated by long periods of silence, while HDC pulses of horseshoe bats (Rhinolophidae) are comprised of longer constant frequency (CF) components ending with a short frequency-modulated (FM) component, and are separated by short periods of silence (Fenton et al., 2012; Jones, 1999; Lazure and Fenton, 2011). Both HDC and LDC echolocators emit pulses at high intensities to ensure the pulse reaches their target at distances that allow the bat sufficient time to maneuver while hunting. However, to avoid self-deafening, LDC echolocators contract the ear muscles (Wever and Vernon, 1961). Once the call is emitted, the ear muscles relax, allowing the bat to hear the returning echo

(Henson, 1965; Suga and Jen, 1975). Thus, LDC echolocators must separate their pulses with sufficient time to allow the echo to return to the ear when the ear muscles are relaxed and their ears are again sensitive to sound. Separating echolocation pulses by time has given LDC echolocators flexibility to adjust the peak frequency (pulse with the strongest energy), bandwidth, intensity, and duration of the pulses (Jakobsen and Surlykke, 2010; Surlykke et al., 2009). For example, increasing the intensity of the pulse increases the detection distance of the pulse, and increasing the bandwidth can increase both the detection distance and resolution of the pulse (Boonman and Ostwald, 2007; Brinkløv et al., 2010; Holderied et al., 2005; Jakobsen et al., 2013). This plasticity has allowed LDC echolocators to occupy a wide range of habitats and use a variety of foraging strategies, which influences their echolocation strategies. For example, LDC echolocators can forage by aerial hawking in open spaces above and below vegetation, trawl fish from water surfaces, and glean prey from the leaves and ground (Fenton, 1995; Neuweiler, 1990). This diversifies their diets, allowing LDC echolocating bats to be insectivorous, piscivorous, frugivorous, nectivorous, carnivorous, sangivorous, and omnivorous (Schnitzler et al., 2003).

In contrast, HDC use a clutter resistant echolocation system in which an acoustic fovea is combined with Doppler-shift compensation and acoustic glints generated by the fluttering wings of insects to detect prey in dense vegetation (Fenton et al., 2012). The acoustic fovea is the region in a HDC bat's auditory cortex with neurons particularly sensitive to a narrow range of frequencies that a bat can hear (Schuller and Pollak, 1979). Because bats echolocate while in flight, their returning echoes are higher in frequency than the emitted pulse due to the Doppler effect. To ensure that the echo returns at a frequency within the range of the acoustic fovea, bats emit pulses at slightly lower frequencies than those to which the acoustic fovea is tuned, so that the returning echo falls within the range of their acoustic fovea (Schnitzler, 1968) as a result of the Doppler effect. This phenomenon is called Doppler shift compensation (DSC). The frequency of the CF component of the emitted pulse of a stationary bat is called the resting frequency (RF), which is also the frequency of the acoustic fovea (Jacobs and Bastian, 2018). DSC is a unique strategy that allows HDC bats to echolocate in areas that are densely vegetated (Bell and Fenton, 1984). Auditory masking effects, whereby the detection of a sound is influenced by the presence of another sound, can be affected by both the overlap of a bat's echolocation call and returning echo (forward masking) and the echoes by the target and the background (backward masking) (Kalko and Schnitzler, 1993). HDC bats avoid forward masking due to DSC, because the emitted echolocation pulse falls outside of their acoustic fovea. Similarly, the separation of the emitted pulse and the echo with time allows LDC bats to avoid forward masking. To avoid backward masking effects, HDC bats have developed the ability to detect acoustic glints from the wingbeats of flying insects. "Glints" are defined as "prominent amplitude peaks in the echo" (Schnitzler and Kalko, 2001) and result when the wing of a moth is perpendicular to the sound wave emitted to the bat (Schnitzler, 1990). These glints result in a ±2 kHz in the broadening of the constant frequency component of the bat's call, dependent on whether the target's wings are facing towards or away from the approaching bat (Schnitzler and Denzinger, 2011). DSC generates a constant echo from the background clutter, and the wingbeats of insects generate slight changes in the frequency of the echo. These glints are superimposed on the CF component of the echo reflected by the insect's body (Fenton et al., 2012; Schnitzler and Denzinger, 2011). This strategy allows HDC echolocating bats to hunt in highly cluttered environments, due to their ability to quickly and accurately detect movement against the constant echo from the background (Bell and Fenton, 1984). Combined, the acoustic fovea, DSC, and acoustic glints generated by the flapping wings of insects against the constant echo of the background, make HDC bats clutter specialists.

The surrounding environment also plays an important role in determining the success of an echolocation pulse (Jones and Holderied, 2007). Sound is propagated through the atmosphere and conditions of the atmosphere, such as temperature, pressure, and humidity, influence sound traveling through the atmosphere. The energy of higher frequency pulses is more readily attenuated by the atmosphere than that of low frequency sound (Lawrence and Simmons, 1982; Luo et al., 2014; Stilz and Schnitzler, 2012). Furthermore, hotter and more humid environments more rapidly attenuate sound because of the absorption of the sound waves by the air and water molecules in the air (Attenborough, 2008). The efficacy of bat pulses is therefore highly dependent on the pulse parameters and the conditions of the atmosphere in which the bats are echolocating. Bats must be able to emit pulses at either lower frequencies within their physiological range, at higher intensities, or a combination of both to ensure the pulse will reach their target and be reflected as an echo audible to the bat (Schuchmann and Siemers, 2010; Surlykke and Kalko, 2008).

The highly specialized nature of HDC pulses put these bats at risk with adapting to environmental change. While LDC bats are able to shift the frequency of their pulses within a certain range, HDC bats are more constrained in this ability due to their acoustic fovea (Jacobs and Bastian, 2018). Doppler shift compensation involves a 2-3 kHz change in frequency (Zhang et al., 2019). Greater changes that these would shift the returning echo outside of the frequency range of the acoustic fovea rendering the echolocation system dysfunctional. Because the attenuation of sound is affected by numerous environmental variables, including air temperature, humidity, and atmospheric pressure, any changes to these variables could affect the prey detection volume and detection distance of echolocating bats (Attenborough, 2008). More specifically, increases in ambient temperature will result in are more readily absorbed high-frequency calls, potentially decreasing a bat's detection range and affecting a bat's ability to hear the returning echo of its prey. Luo et al. (2014) projected that climate change will alter the prey detection volume (measure of the size of 3-dimensional space within which a bat detects prey) of bats depending on call frequency. Prey detection is the maximum volume that a bat can detect while foraging for prey (Luo et al., 2014)**.** Bats that echolocate at lower frequencies may see increases in their prey detection volumes, while bats that echolocate at high frequencies will see reductions (Luo et al., 2014). However, I only used climate projections to predict potential changes in prey detection volume. The prey detection volume between bats of the same species living in environments with different ambient temperatures are currently unknown. Furthermore, studies on the prey detection volume of bats typically use resting frequency as the most important indicator for how bats can perceive their surroundings. While this is a significant parameter, it is important to note that prey detection volume relies on detection distance. Detection distance in turn relies on the emitted intensities (source level), atmospheric conditions, frequency, and hearing sensitivity (Surlykke and Kalko, 2008). Reductions in prey detection volume of bats due to climate change could have serious consequences, including higher energy expenditure while foraging, longer periods of torpor, reduced reproduction rates, and population stresses (Barclay, 1991; Bronner et al., 1999; Sherwin et al., 2013; Stawski and Geiser, 2010).

I will examine the potential effects of ambient temperature on the Cape horseshoe bat, *Rhinolophus capensis*. While there is variation in some biological traits of *R. capensis*, such as resting frequency, wing size, and body mass, no sub-species of *R. capensis* have been described, and gene flow still exists between these populations (Dool et al., 2016; Odendaal and Jacobs, 2011). Horseshoe bats belong to the family Rhinolophidae, and inhabit diverse regions of Europe, Africa, Asia, and Australia. They are HDC echolocators, which constrains their echolocation plasticity (Bastian and Jacobs, 2015). They also have documented variation in their wing sizes and shapes across their range, which could potentially correspond with their thermoregulatory needs (Odendaal and Jacobs, 2011). *Rhinolophus capensis* is ideal for this study because it has a wide geographic distribution in South African occupying a range of biomes from Desert to southern Afrotemperate Forest (Monadjem et al., 2011).

Changes in the prey detection volume of echolocating bats could potentially lead to selection for different wing shapes and size due to the adaptive complex between echolocation and wing shape. (Arita and Fenton, 1997; Lancaster et al., 1997; Norberg and Rayner, 1987). I examined how *R. capensis*' prey detection volume and wing shape is affected by the different climates across its geographic distribution as a means of gauging how predicted climate change is likely to impact this species of bats.

If climatic differences do have an impact on both wing area and echolocation parameters, this should be reflected in differences in the relative wing area and prey detection volumes of *R. capensis* across its distribution. Specifically, if wings are important for thermoregulation, *R. capensis* should have relatively larger wings in hotter, more arid regions of its distribution. If prey detection volume is influenced by ambient temperature, *R. capensis* should have lower prey detection volumes in warmer climates due to the effects of atmospheric attenuation. Luo et al. (2014) that increases in ambient temperature will lead to reduced prey detection volumes for bats that echolocate above 40 kHz when global climate increases 2˚C, and approximately 90 kHz when global climate increases 4˚C. Because *R. capensis* echolocates at a frequency between 75 and 86 kHZ (Odendaal and Jacobs, 2011), I predicted that their prey detection volumes will be reduced in populations living in hotter climates, potentially leading to a decrease in their ability to find and consume prey (Luo et al., 2014).

METHODS

ETHICS STATEMENT

This study involved the capturing and handling of live animals in the field. This study received animal ethics' clearance from the University of Cape Town animal ethics committee (Permit no: 2018/v13/DJ). I obtained permits from each of the sites where data were collected (CN44-59-7163; FAUNA 0912/2018; FAUNA 0913/2018). Upon capture, I placed each bat in a cotton bag to ensure they would not get hypothermic or hyperthermic. I gave each bat water and handled them swiftly and carefully to minimize the stress experienced by the animal. Bats were released the subsequent evening after capture at the point of capture. No threatened species were handled.

STUDY SPECIES

Rhinolophus capensis (12.0 g ± 1.7 g) is a medium sized insectivorous bat found across southern Africa (Jacobs and Bastian, 2018; Stoffberg, 2008; Taylor et al., 2018). They have a coastal distribution extending from the Orange River in the northwest of South Africa, an extremely arid region, down to southern tip of South Africa, known for its prevalent fynbos vegetation, and eastwards to the Eastern Cape Province, well-known for its dense forests. *Rhinolophus capensis* typically roosts in abandoned mines or caves, often with *Rhinolophus clivosus* and *Miniopterus schreibersii natalensis* (Stoffberg, 2008). *Rhinolophus capensis* forages in cluttered habitats, and has short, broad wings allowing maneuverable flight at slow speeds (Jacobs et al., 2007; Norberg and Rayner, 1987). They are characterized as perch-hunters, and feed on moths and other flying insects (Aldridge and Rautenbach, 1987; Jacobs et al., 2007; Stoffberg, 2008). *Rhinolophus capensis* is a HDC echolocator, whose pulses are comprised of a long constant frequency component with short, modulated frequency components (Stoffberg, 2008). The peak frequency of *R. capensis* calls varies across its distribution. *Rhinolophus capensis* emits low frequency calls (75kHz) in the northwest part of its range, and higher frequency calls in the southeast part of its range (86 kHz) (Odendaal et al., 2014).

DESCRIPTION OF STUDY SITES

I conducted field work to collect echolocation data and wing images between February and November 2019. I analyzed wing images collected from previous field work conducted in 2007, 2008, 2010, and 2018 by David Jacobs and the students in his group to increase sample sizes. I also analyzed echolocation data from field work conducted in 2017 and 2018. The data were also recorded using the same methods as I used in this study.

I collected wing images from 9 study sites across South Africa including Lekkersing (-28.42 º, 16.88 º), Steenkampskraal (-30.98 º, 18.63 º), Zoutpansklipheuwel in the Karoo (-31.63 º, 18.21 º), Heidehof (-34.42 º, 20.63 º), De Hoop Nature Reserve (-34.42 º, 20.36 º) Knysna (-33.88 º, 23.00 º), Baviaanskloof (-33.63 º, 24.24 º), Sleepy Hollow (-33.96 º, 25.28 º), and Table Farm (-33.28 º, 26.42 º) (Odendaal and Jacobs, 2011). Echolocation data were recorded from 5 sites, including Lekkersing (-28.42 º, 16.88 º), Zoutpansklipheuwel (-31.63 º, 18.21 º), De Hoop (-34.42 º, 20.36 º), Baviaanskloof (-33.63 º, 24.24 º), and Table Farm (-33.28 º, 26.42 º). I took latitude and longitude coordinates using a handheld Garmin GPS (model Colorado, Garmin International INC, Kansas, USA). These 9 sites cover 7 ecoregions and provide a comprehensive sample (Figure 1). Ecoregion information was obtained from Dinerstein et al. (2017).

Lekkersing, Steenkampskraal, and Zoutpansklipheuwel are part of the Namaqualand-Richtersveld steppe ecoregion, with Steenkampskraal bordering the succulent Karoo xeric shrubland ecoregion (Dinerstein et al., 2017). These ecoregions are both part of the Succulent Karoo biome, which is dominated by a diverse range of low-lying succulent plants (Mucina et al., 2006b). The area sampled around Lekkersing is near the Orange River, which is classified as a winter-rainfall desert, whereas the areas around Steenkampskraal and Zoutpansklipheuwel have more moderate climates (Rutherford et al., 2006). Lekkersing has an average yearly rainfall of 67 mm, and an average monthly air temperature between 15 °C and 24 °C (Hersbach et al., 2020; Lobelia, 2020). Steenkampskraal has an average yearly rainfall of 165 mm, and an average monthly air temperature between 13 °C and 23 °C (Hersbach et al., 2020; Lobelia, 2020). Zoutpansklipheuwel has an average rainfall of 177 mm, and an average monthly air temperature between 13 °C and 21 °C (Hersbach et al., 2020; Lobelia, 2020). Heidehof and Sleepy Hollow are part of the Fynbos shrubland ecoregion. Most fynbos in this ecoregion are part of the Restionaceae, Proteaceae and Ericaceae families (Rebelo et al., 2006). Fynbos in these families are characterized as small shrubs with evergreen leaves, and have very high rates of endemism (Rebelo et al., 2006). Heidehof has an average yearly rainfall between 576 mm, and an average monthly air temperature between 12 °C and 20 °C (Hersbach et al., 2020; Lobelia, 2020). Sleepy Hollow has an average yearly rainfall of 711 mm, and an average monthly air temperature between 13 °C and 20 °C (Hersbach et al., 2020; Lobelia, 2020). De Hoop is part of the Renosterveld shrubland ecoregion (Dinerstein et al., 2017). While both the Fynbos shrubland and the Renosterveld shrubland are part of the greater Fynbos Biome, which has a Mediterranean climate, the Renosterveld is dominated by fynbos from the Asteraceae family and grasses (Rebelo et al., 2006). De Hoop has an average yearly rainfall of 379 mm, and has an average monthly temperature between 13 °C and 22 °C (Hersbach et al., 2020; Lobelia, 2020). Knysna is part of the Knynsa-Amatole mountain forest ecoregion (Dinerstein et al., 2017). This ecoregion has a warm climate, with high concentrations of fynbos, dense Afromontane forests, and Milkwood forests (Mucina et al., 2006a). Knysna receives an average yearly rainfall of 701 mm and a monthly average temperature between 13 °C and 20 °C (Hersbach et al., 2020; Lobelia, 2020). Baviaanskloof is a highly diverse region. The area sampled straddles the Renosterveld shrubland and Albany thicket ecoregions, and is surrounded by the Fynbos shrubland ecoregion (Dinerstein et al., 2017). This entire area, however, encompasses 7 out of 8 biomes represented in South Africa (Rutherford et al., 2006). The Albany thicket is dominated by dense, woody thickets (Hoare et al., 2006). Baviaanskloof has an average yearly rainfall of 589 mm and monthly average temperatures range from 11 °C to 20 °C (Hersbach et al., 2020; Lobelia, 2020). Finally, Table Farm straddles the Fynbos shrubland and Albany thicket (Dinerstein et al., 2017). It has an average yearly rainfall of 618 mm and monthly average temperatures range from 13 °C to 21 °C (Hersbach et al., 2020; Lobelia, 2020). Although rainfall variation was the greatest between sites, this study was focused on the impacts of changing temperatures due to climate change, so this variable was not considered.

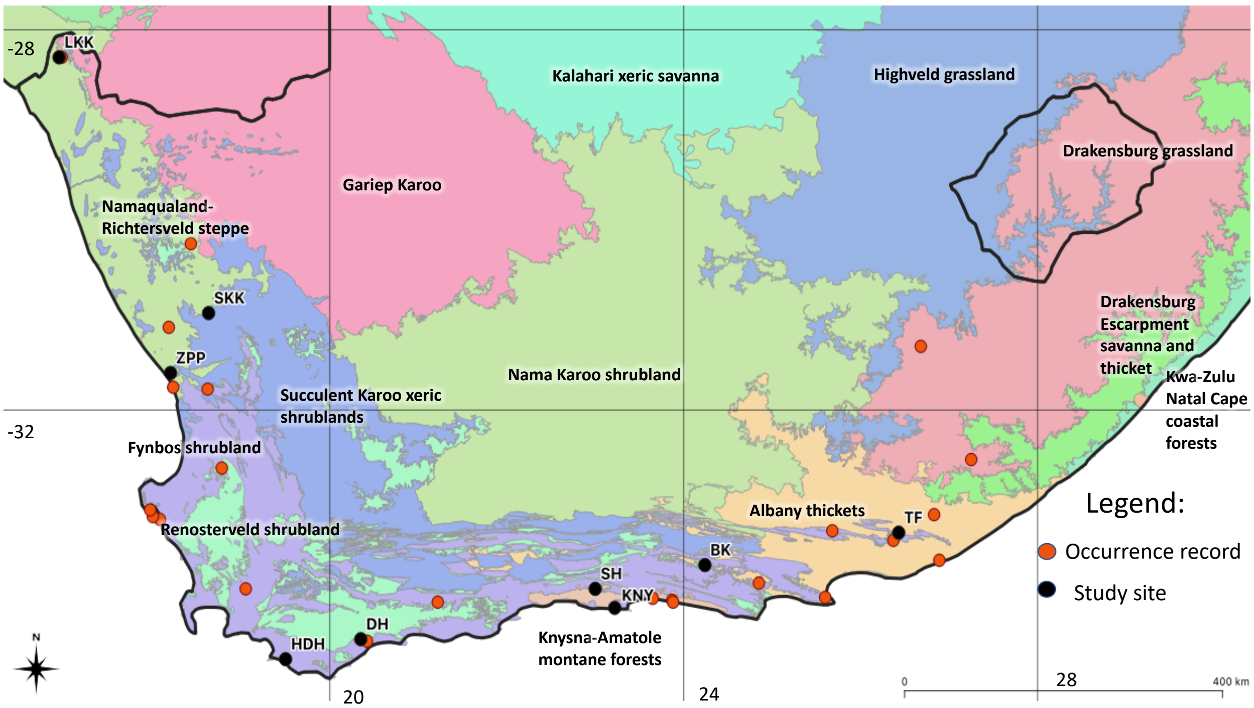

FIGURE 1: A map showing the ecoregions, study sites, and occurrence records of *R. capensis* across South Africa. Wing area data of *R. capensis* was taken at each of the study sites, and echolocation data was taken at 5 of these sites. Occurrence record data taken from Bernard (2011). Ecoregion data taken from Dinerstein et al. (2017).

(Abbreviations: LKK= Lekkersing; SKK = Steemkampskraal; ZPP= Zoutpansklipheuwel; HDH= Heidehof; DH= De Hoop Nature Reserve; SH= Sleepy Hollow; KNY= Knysna; BK= Baviaanskloof; TF= Table Farm)

ENVIRONMENTAL DATA

I took environmental data from each of the 9 sites across the *R. capensis* range in southern Africa. *Rhinolophus capensis* are distributed in several major biomes that experience a wide range of rainfall patterns and are characterized by differences in the vegetation cover. These habitats also experience noticeable differences in average temperature and average humidity. Because evolutionary change is likely driven by the "extreme" conditions of an environment, this analysis used climatological maximum means from the summer months (December, January, and February) and the climatological minimum means from the winter months (June, July, and August) between 1979 and 2019 (Araújo et al., 2013; Kearney et al., 2013) To quantify the seasonal maximum and minimum mean temperatures of each of these environments, I used ERA5 atmospheric reanalysis data. ERA5 uses data assimilation to combine observational and model data to compile optimal atmospheric climate data measurements (Hersbach et al., 2020). The spatial horizontal resolution is 31 km. Given that the closest weather stations to each of my study sites was up to 100 km away, and sometimes in entirely different ecoregions, ERA5 data are likely to provide a more accurate characterization of atmospheric climate conditions over the 40 years between 1979 and 2019 (Hersbach et al., 2020).

WING MORPHOLOGY

To test the prediction that wing area has a positive relationship with temperature, I captured *R. capensis* at night after returning from foraging using mist nets and a harp trap. I released nursing and pregnant mothers and juveniles to eliminate any differences in mass due to pregnancy or stage of development. Bats were kept overnight in cotton bags to ensure no differences in weight were due to variations in the amount of food eaten the previous night. I measured weight to the nearest 0.01 g using an electronic balance scale (Ohaus Scout Pro SPU402, OHAUS Corporation, Pine Brook, New Jersey, USA). I recorded sex and age of the bats. Age was determined by observing wing-bone ossification, specifically looking at the transparency of the epiphyseal growth plates (Anthony, 1998). Adults have non-visible epiphyseal plates. I measured forearm length using dial calipers (Model MDC-6, Taylor Toolworks, Columbia, Missouri, USA) and photos of wings were taken to determine wing area.

The bats were placed over graph paper so that the software used to measure the outstretched right wing could be calibrated, and the photographs were taken directly over the wing. I digitally photographed wings using SAMSUNG Galaxy A7 (SM-A750FZBAXFA) produced by SAMSUNG Electronics (Samsung Digital City, Samsungno 129, Yeongtong District, South Korea). A primary 24 megapixel f/1.7 sensor was used.

I analyzed digital images of the wings using SigmaScan Pro 5 software (Version 3.20, SPSS, IBM, USA). After calibrating the software using the calibrate distance and area menu option, I measured the area of half of the body, the plagiopatagium (right arm- wing), the dactylopatagium (right handwing), and half of the tail membrane, in that order. I then added these measurements and multiplied the value by 2 to generate the total wing area. I then used the total wing area measurements in the subsequent statistical tests.

ECHOLOCATION DATA

To test the prediction that prey detection volume has a negative relationship with temperature, I used a microphone array system to gather echolocation data. The array system converts sound pressure into electronic signals (Simmons, 2014). It consisted of four Knowles FG-O omnidirectional electret microphones arranged on each of two separate star arrays (Figure A1 in a symmetric pattern (Avisoft Bioacoustics, Germany). The two arrays were positioned approximately 1-1.5 m apart from each other near the entrance of the caves and mines to capture calls from bats exiting from their roosts to forage. The arrays were placed perpendicularly to the observed flight paths of the bats. Arrays were level with the ground and to each other to ensure accurate triangulation of the bats' flight path. Echolocation calls were recorded at a sampling rate of 300 kHz using an AviSoft UltraSoundGate 816H (Avisoft Bioacoustics, Germany), which was connected to a Dell laptop (Model: Latitude E7240, Texas, USA). Echolocation pulses were recorded for 1-2 hours after bat emergence on nights with no rain and low wind speeds. Recording would be manually triggered and saved when high quality pulses appeared on the computer screen.

All pulses were initially analyzed using AviSoft software (Avisoft SASLAB Pro Version 5.2.09, Germany). To determine that pulses were coming from *R. capensis*, I calculated peak frequency using the “Spectrogram parameters” function in AviSoft. I analyzed the shape of the call to ensure that it was an HDC pulse. I also recorded the average frequency of the set of pulses for subsequent analysis. Only quality pulses (i.e. those with clear FM and CF components in an uninterrupted sequence and high signal to noise ratio) were analyzed. All background noise, sequences with multiple pulses recorded at once, and atypical pulses were eliminated prior to analysis by using the “erase” function in AviSoft software.

The time of arrival (TOA) at each microphone of an echolocation pulse emitted by a bat flying in the vicinity of the arrays would be different. I calculated TOA differences among the eight microphones using cross-correlation code developed by Holderied and Von Helversen (2003) in MATLAB 8.1 (The Math Works Inc., Natick, Massachusetts, USA). The code was written by Dr. Marc Holderied and permission for its use was granted for this study. I removed the CF component of the echolocation pulses and background noise using a custom-made script, leaving only the FM component of the pulse. I applied the cross-correlation function to the FM components only. The script allowed the bat’s position to be plotted when the bat emitted each echolocation pulse and these positions were used to reconstruct the bat’s flight path relative to the two arrays. Not all pulses included in the flight path necessarily came from the same bat, and at times two or more pulses would be superimposed on the same position. Because I was recording at dusk when many bats were exiting their roosts to forage, it was not uncommon to record multiple bats at once. Thus, I deleted pulses until a smooth flight trajectory was obtained with one bat flying towards the microphone array systems. I only used the pulse with the maximum source level at microphones 1 or 5 in the calculation of detection volumes (dBs). The maximum source level is most likely received when the bat is closest to being online with the axis of the microphones, making it the most reliable indicator of source level. Source level is expressed in decibels (dB) per sound pressure level (peSPL) (Holderied and Von Helversen, 2003)

I used a weather station (Professional Weather Center, Model WMR200A, Oregon Scientific, Inc., Tulatin, Oregon, USA) to gather environmental temperature, humidity, wind speed, and atmospheric pressure data at the time echolocation pulses were recorded. These variables were necessary to calculate the atmospheric attenuation of the energy in each pulse so that the source levels at 10 cm from the bat for each pulse could be determined and extrapolated from the voltage registered at the center microphone of each array when the pulse reached this microphone.

To calculate the detection range of an echolocation pulse, it is necessary to calculate the attenuation of this sound in air. Sound attenuation in air depends on multiple environmental factors including humidity, atmospheric pressure, and air temperature, and sound frequency. I calculated the attenuation of the echolocation pulse according to the ISO9613-1 standard (ISO, 1996) as follows:

EQUATION 1

$$\alpha_{iso} = 8.686 \times f^2 \times \sqrt{\tau} \times \frac{(1.84\times10^{-11})}{p_r + \tau^{-3} \times (b_1 + b_2)}$$

Input arguments to
Equation 1 are as follows:

EQUATION 2

$$\tau = \frac{T}{T_0}$$

where τ is the ratio of the ambient temperature T to the standard temperature T_0 (293.15K)

EQUATION 3

$$p_r = \frac{p_s}{p_{s0}}$$

where p_r is the pressure ratio of the ambient pressure p_s to standard pressure p_{s0} (1.0 atm)

EQUATION 4

$$h_{iso=\, h_r \times} \frac{p_{sat_{ps0_{iso}}}}{p_r}$$

where h_{iso} is the humidity in percent molar, h_r is relative humidity and $p_{sat_{ps0_{iso}}}$ is the saturation pressure ratio according to ISO, given by:

EQUATION 5

$$p_{sat_{ps0_{iso}}} = 10^{\varphi}$$

and

EQUATION 6

$$\varphi = -6.8346 \times \left(\frac{273.15}{T}\right)^{5.8761}$$

EQUATION 7

$$f_{r0} = p_r \left(\frac{24 + 40400 \times h_{iso} \times (0.02 + h_{iso})}{0.391 + h_{iso}}\right)$$

EQUATION 8

$$f_{rN} = p_r \left(\frac{1}{\sqrt{\tau}} \times (9 + 280 \times h_{iso} \times e^{\left(-417 \times \left(\frac{1}{\sqrt[3]{\tau}}\right) - 1\right)}\right)$$

EQUATION 9

$$b_1 = 0.1068 \times e^{\left(\frac{-3352/T}{f_{rN} + f^{\frac{2}{f_{rN}}}}\right)}$$

EQUATION 10

$$b_2 = 0.01275 \times e^{\left(\frac{-2239.1/T}{f_{r0} + f^{\frac{2}{f_{r0}}}}\right)}$$

These computations were coded in MATLAB and are available online (Zechmann, 2020). I obtained attenuation values by inputting field recordings of average frequency for microphones 1 and 5, temperature, pressure ratio (ambient to standard) and relative humidity. Climate values were measured using the weather station while the echolocation frequencies were recorded.

I calculated detection distance using the same method as Stilz and Schnitzler (2012). I used a custom-built MS Excel spreadsheet (Version 16.0.13628.20128, Washington, USA) which solved for detection distance after inputting source level and sound attenuation (decibels per meter) (Table A1). This spreadsheet was created by Nikita Finger and permission was granted to use this spreadsheet for this study. Since prey detection volume success also depends on the size of the prey, it was necessary to consider target strength in this equation. I used three target strengths (-40 dB, -50 dB, and -65 dB) to estimate the approximate signal echo from small, medium, and large prey. -65 dB corresponds to small prey items, -50 corresponds to medium-sized prey items, and -40 corresponds to large prey items. These are estimates of the approximate target strength for months typically eaten by *R. capensis*. I used a detection threshold of 20 dB following Stilz and Schnitzler (2012). Using these values, the Excel solver calculated the detection distance of bats (d) when searching for small, medium, and large prey using the function

EQUATION 11

$$\Delta L(d) = C_1 + C_2 \cdot log_{10}(d/d_{ref})$$

where ΔL (d) refers to the attenuation in decibels over logarithm of distance, C_1 accounts for the energy reflected, and C_2 accounts for the energy lost due to spreading. These values were estimated (Stilz and Schnitzler, 2012).

I measured prey detection volume using Luo et al.'s model (Luo et al., 2014). Luo et al. (2014) calculated the values for perch-hunting and flying bats separately. Because the microphone array system did not allow me to identify individual bats, only the flight paths of bats passing the arrays, changes in the prey detection volume while in flight could not be calculated. Even though R. *capensis* hunts in flight, I used the equation used to calculate the prey detection volume of perch-hunting bats (Stoffberg, 2008). The equation for bats hunting in flight takes into account the overlap of the detection beams as the bat approaches its target (Luo et al., 2014). The equation for perch-hunting bats, however, still provides a good indication of the detection volume of R. *capensis* from a single call, since I was unable to calculate the overlap of the detection beams of R. *capensis*. Volume (V) is defined as follows:

EQUATION 12

$$V = \frac{2\pi d^3}{3}\,(1 - \cos\frac{\theta}{2})$$

Where d is defined as the maximum prey detection distance (radius of the sphere) and θ is defined as the full width of the sonar beam. The width of the sonar bean is determined by the size of the bat's emitter (mouth or nostrils) and the frequency of the emitted pulse (Strother and Mogus, 1970; Urick, 1983). For example, a sonar beam with higher directionality can result from the widening of the mouth or a higher frequency pulse (Jakobsen et al., 2013; Surlykke et al., 2009). If intensity remains constant, broader beams decrease detection distance, and narrower beams increase detection distance (Jakobsen et al., 2013). At constant frequencies, higher intensity calls result in a greater detection volume (Surlykke et al., 2009). I calculated "d" using the equation from Stilz and Schnitzler (2012) as described above. During this analysis, each of the target strengths of -40 dB, -50 dB, and -65 dB were considered. Based on Matsuta et al. (2013), I used a beam width of 22 °. In their study, the beam width of *Rhinlophus ferrumequinum* ranged between 22 ° ± 5 ° (Mean ± SD) during the search phase. Since I wanted to understand the prey detection volume of R. *capensis* during flight, using the average beam width during the search phase of flight was most practical. No other studies have analyzed beam widths of rhinolophid bats, so Matsuta et. al. (2013) provided the most reasonable estimate of beam width for a rhinolophid.

DATA AND STATISTICAL ANALYSIS

To determine if a relationship exists between wing area and temperature, I used a linear mixed-effects model. A linear mixed effects model also takes into account other variables that may influence wing area. Biological predictor variables included body mass and sex. It was important to include sex in the models because there might be different degrees of sexual dimorphism in each population and it is relative wing area that is relevant here. Body mass and wing area are correlated and larger bats may have larger wings to decrease wing loading (Norberg and Rayner, 1987). This could lead to the false conclusion that climate drives wing area, whereas body size may be responding to selection pressure with an allometric response by the wings. However, both wing loading and body mass could not be considered together given the collinearity between the variables (Norberg and Rayner, 1987). Sexual dimorphism in body size has been observed in *R. capensis* (Odendaal and Jacobs, 2011). Populations from which a higher number of one sex was sampled may spuriously lead to the conclusion that the population has relatively larger wing areas. I did not include forearm length as a proxy for body size because of possible correlations between forearm length and wing area. Body mass is a reliable indicator of body size in *Rhinolophus capensis*, despite possible seasonal and diurnal changes in their masses (Odendaal and Jacobs, 2011), provided bats are measured at the same developmental stage, at the same time of day and after the digestive system has been voided. Since bats were given sufficient time to empty their digestive systems after their initial capture, diurnal body mass variation was controlled (Odendaal and Jacobs, 2011). I did not analyze pregnant females and sampling was only done in the spring and summer months, controlling for seasonal changes in body mass. I gave water to each individual bat before they were measured and weighed to control for dehydration mass loss.

I included latitude as a spatial predictor because latitude is correlated with global climactic patterns. Because the Lekkersing population was over 2 º further north than the next closest site, Steenkampskraal, latitude can be used to determine if differences between wing area and prey detection volumes between sites is correlated with global climactic differences. Furthermore, genetic drift may lead to morphological changes across the distribution of *R. capensis*. This variable accounts for any spatial divergence that could be observed in the population. Furthermore, environmental predictors include summer maximum temperature, summer minimum temperature, winter maximum temperature, and winter minimum temperature from the ERA5 data set. I included normalized difference vegetation index (NDVI) as an environmental variable to account for differences in wing area and prey detection volume in response to clutter. NDVI is particularly useful to look at landscape change, and Pettorelli et al., (2005) found that it was particularly useful in distinguishing between savannas, forests, and agricultural fields. Since there is a documented relationship between clutter, wing shape, and echolocation pulse design, I expected to see a relationship between these variables (Aldridge and Rautenbach, 1987; Norberg and Rayner, 1987). NDVI is calculated using the equation:

EQUATION 13

$$NDVI = \frac{NIR - Red}{NIR + Red}$$

where NIR is defined as the spectral reflectance measurements in the near-infrared region, and Red is defined as the spectral reflectance measurements in the visible region. NDVI values range between -1 and +1, with -1 values corresponding to areas with an absence of vegetation (e.g. desert), and +1 corresponding to areas with dense vegetation (e.g. forest). Vegetation rich in chlorophyll and/or highly dense absorb more Red and NIR light. I used NASA's MODIS dataset, downloaded using the MOD13Q1 product (Didan, 2015). This allows users to extract 16 day NDVI averages with a resolution up to 250 m from 2001 to the present. I calculated NDVI for each of my sites by averaging the values from 2001 to 2020 with a 20 km radius around each site. The NDVI data set spans from 2001 to 2020, and all of these data were used.

I created a linear mixed-effects model to determine if a relationship exists between prey detection volume and temperature, using prey detection volume as the dependent variable and average summer maximum, average summer minimum, average winter maximum, and average winter minimum temperatures from 1979 to 2019. I analyzed each environmental variable in separate models to avoid any possible collinearity. I included latitude (decimal degrees) as a spatial predictor.

Because the microphone arrays record flight paths of bats, it was not possible to collect individual information from the bats recorded. Body size and sex were not therefore taken into account during the analysis of prey detection volume in each locality. Based on observations during the data collection period, multiple bats flew past the microphone array systems. Thus, it is reasonable to assume that data were collected from multiple individuals. I included locality as a random effect in the models to account for variation in samples sizes across sites. Separate models for each target strength (-40 dB, -50 dB, and -65 dB) which included each combination of environmental variables were generated.

Model selection was determined by the lowest corrected Akaike information criteria (AICc) score (between 2054.8 and 2067.1 for wing area and 1966.7 and1978.5 for prey detection volume) (Akaike, 1998). I ran a total of 80 linear mixed-effects models to test the prediction that wing area would have a relationship with temperature and to see which combination of biological, spatial, and environmental variables best explained differences in wing area across localities. The random effect of locality was included in each of the models to account for the multiple individuals sampled at each site. I ran the models with and without locality as a random effect. However, based on the AICc scores, locality as a random effect had a significant effect on reducing AICc, and was thus included in all models run.

For the prey detection volume analysis, there was a total of 19 different combinations of biological, spatial, and environmental predictors. This amounted to a total of 57 models for each target strength. Again, I ran each combination of predictors and response variables to determine those which best explained differences in prey detection volume. The random effect of locality had a significant effect on lowering the AICc score and was included in each of the models. Because *R. capensis* is most likely to catch and eat small prey given its size (Jacobs et al., 2007), and because this set of models had the lowest AICc values, only the results for prey detection volume calculated with a target strength of -65 dB are displayed.

I selected the model with the lowest AICc score. AICc takes into account the sample size and amount of variables (K) being used to explained the response variable (Akaike, 1998). I determined differences in AICc score and between each model and evidence ratios to estimate the explanatory value of the models in relation to the others (Maluleke et al., 2017).

I generated the linear mixed models and figures in MATLAB (Version 8.1). I ran each model using the “fitlme” script in MATLAB.

To determine if there was normality in the wing area and prey detection volume data sets, I ran a Kolmongrov-Smirnos test using SPSS (Version 26, IBM, USA). I created a histogram of the residuals and residuals versus fits plot using MATLAB. I checked for heteroskedasticity in the wing area data set by running a Levene’s test in SPSS. I created a residual scatterplot in MATLAB. All model validation figures were created using the “plotResiduals” script in MATLAB. Given the heteroskedasticity of the wing area data, which failed to meet the assumptions of an ANOVA test, I used a Kruskal-Wallis test to assess differences between the sites. Similarly, the prey detection volume data set failed the normality and heteroskedasticity assumptions, so I ran a Kruskal-Wallis test to determine differences between sites. I ran a Dunn’s post hoc test for both data sets to determine which sites differed from each other. I ran a Spearman’s rank order correlation test in SPSS to determine correlation between each of the environmental, spatial, and biological variables. All tests used an alpha value of 0.05

To check for outliers within each of the sites, I used the Tukey method. I calculated the interquartile range (IQR) of the data at each site, for both prey detection volume and wing area. High outliers values were calculated using the equation:

EQUATION 14

$$Q_3 + 1.5\ \mathrm{IQR}$$

Low outliers were calculated using the equation

EQUATION 15

$$Q_1 + 1.5\ \mathrm{IQR}$$

I found one high outlier in the wing area data set, and it was eliminated from the analysis. I found high outliers and low outliers for prey detection volume, but I did not eliminate these values from the analysis. They did not significantly affect the statistical analysis. Furthermore, the average values for source levels for each of the sites fell within an expected range of source levels for *R. capensis* (Surlykke and Kalko, 2008).

RESULTS

WING AREA

I analyzed a total of 260 bat wing images collected from 9 localities between 2007 to 2019. Lekkersing had the highest average wing area and Sleepy Hollow had the lowest average wing area (Table 1).

TABLE 1: Ecoregion, wing area, resting frequency, body mass, and prey detection volume of *R. capensis* by locality. Localities are in order of decreasing latitude.

Locality	Ecoregion	Wing Area (mm^2) (n) (Mean ± SD)	Resting Frequency (kHz) (Mean ± SD)	Mass (g) (Mean ± SD)	Prey Detection Volume (dB) (Mean ± Standard Deviation)		
					TS: -40	TS: -50	TS: -65
Lekkersing	Namaqualand-Richtersveld steppe	(7) 175. 77 ± 15.08	74.7 ± 0.4	12.96 ± 3.19	614.85 ± 317.99	366.53 ± 212.59	153.09 ± 106.06
Steenkampskraal	Namaqualand-Richtersveld steppe	(22) 161.91 ± 7.39	80.7 ± 0.5	13.15 ± 0.96	-	-	-
Zoutpansklipheuwel	Namaqualand-Richtersveld steppe, succulent Karoo xeric shrubland	(33) 148 ± 12.09	80.8 ± 0.8	13.42 ± 0.80	382.73 ± 89.27	213.47 ± 56.21	75.53 ± 26.29
Table Farm	Fynbos and Albany thicket	(79) 154 ± 14.55	85.28 ± 0.9	12.84 ± 1.37	395.62 ± 81.33	233.69 ± 51.25	91.60 ± 23.74
Baviaanskloof	Fynbos shrubland, Renosterveld shrubland, Albany thicket	(27) 158.55 ± 11.03	85.04 ± 1.4	10.71 ± 1.39	303.20 ± 126.33	172.76 ± 81.40	64.59 ± 37.15
Sleepy Hollow	Fynbos shrubland	(20) 135.25 ± 10.83	84.50 ± 1.1	12.35 ± 1.47	-	-	-
Knysna	Knysna-amatole mountain forests	(6) 157 ± 12.66	83.33 ± 0.8	11.50 ± 0.55	-	-	-
De Hoop	Renosterveld shrubland	(46) 155.26 ± 10.46	84.60 ± 0.8	10.28 ± 1.08	330.60 ± 132.51	192.07 ± 87.01	74.60 ± 41.81
Heidehof	Fynbos shrubland	(20) 151.64 ± 9.12	83.00 ± 0.5	11.40 ± 0.44	-	-	-

Abbreviations: TS = Target Strength

The most parsimonious mixed-effects model to explain differences in wing area included the fixed effects of body mass, average winter minimum temperature, and sex with the random effect of locality (Table 2). Body mass was included in all of the top models. The top 10 models, which explained more than 40% of the variability, included body mass, sex, and minimum temperature (average winter and average summer).

It is apparent that the best fit model does not sufficiently explain differences in wing area, since its AICc weight is only 5 %. It is also evident that no one model carries significantly more weight in explaining variation in wing area, because the differences in evidence ratios among the top ten models are small (Table 2).

Analysis of the residuals confirms the normality assumption (Figures A11 & A12). The scatterplot of the residuals reveals heteroskedasticity, further suggesting that this model alone may not fully describe differences in wing area (Figure A13).

TABLE 2: Results of the linear mixed effects model testing different combinations of biological, spatial, and environmental variables to best predict variation in wing areas of *R. capensis* across 9 localities in South Africa

Model	K	AICc	Delta AICc	ModelLik	AICc Wt	LL	Cum. wt	ER
Sex + Body mass + avg winter min	5	2054.8	0	1	0.05	-1021.2	0.05	
Sex + Body mass + Lat	5	2054.9	0.1	0.95	0.05	-1021.3	0.08	1.05
Body mass+ avg winter min	4	2054.9	0.1	0.95	0.05	-1022.3	0.14	1.05
NDVI + Sex + Body mass + avg summer min	6	2055.2	0.4	0.81	0.04	-1020.4	0.19	1.22
Body mass+ Lat	4	2055.3	0.5	0.78	0.04	-1022.5	0.22	1.28
Body mass	3	2055.3	0.5	0.78	0.04	-1023.6	0.26	1.28
Sex + Body mass	4	2055.4	0.6	0.74	0.04	-1022.6	0.30	1.35
NDVI + Body mass + avg summer min	5	2055.4	0.6	0.74	0.04	-1021.5	0.34	1.35
NDVI + Body mass	4	2055.5	0.7	0.71	0.04	-1022.7	0.37	1.42
NDVI + Sex + Body mass	5	2055.5	0.7	0.71	0.04	-1021.6	0.41	1.42
Sex + Lat + Body mass + avg winter min	6	2055.7	0.9	0.64	0.03	-1020.6	0.44	1.57

Sex + Body mass + avg summer min	5	2055.8	1	0.61	0.03	-1021.7	0.47	1.65
Body mass + avg summer min	4	2055.8	1	0.61	0.03	-1022.8	0.50	1.65
Sex + Lat + Body mass + avg summer min	6	2055.9	1.1	0.58	0.03	-1020.7	0.53	1.73
NDVI + Sex + Body mass + avg winter min	6	2055.9	1.1	0.58	0.03	-1020.7	0.56	1.73
Body mass + Lat + avg winter min	5	2056.1	1.3	0.52	0.03	-1021.9	0.58	1.92
NDVI + Body mass + avg winter min	5	2056.1	1.3	0.52	0.03	-1021.9	0.61	1.92
Sex + Lat + Body mass + avg summer max	6	2056.7	1.9	0.39	0.02	-1021.1	0.63	2.58
NDVI + Sex + Body mass + Lat	6	2056.9	2.1	0.35	0.02	-1021.3	0.64	2.86
Sex + Lat+ Body mass + avg winter max	6	2057	2.2	0.33	0.02	-1021.3	0.66	3.00
Body mass + Lat + avg summer min	5	2057.1	2.3	0.32	0.02	-1022	0.68	3.16
Body mass + Lat+ avg summer max	5	2057.1	2.3	0.32	0.02	-1022.4	0.69	3.16
Sex, Body mass+ avg summer max	5	2057.1	2.3	0.32	0.02	-1022.4	0.71	3.16
Body mass + avg summer max	4	2057.1	2.3	0.32	0.02	-1023.4	0.72	3.16
NDVI + Body mass + Lat	5	2057.2	2.4	0.30	0.02	-1022.4	0.74	3.32
NDVI + Sex + Body mass + Lat + avg summer min	7	2057.3	2.5	0.29	0.014	-1020.3	0.75	3.48
Body mass + Lat + avg winter max	5	2057.4	2.6	0.27	0.01	-1022.5	0.77	3.66
Body mass + avg winter max	4	2057.4	2.6	0.27	0.01	-1023.6	0.78	3.66
NDVI + Sex + Body mass + avg summer max	6	2057.4	2.6	0.27	0.01	-1021.5	0.79	3.66
Sex + Body mass + avg winter max	5	2057.5	2.7	0.26	0.01	-1022.6	0.81	3.86
NDVI + Body mass + avg summer max	5	2057.5	2.7	0.26	0.01	-1022.6	0.82	3.86
NDVI + Body mass + Lat + avg summer min	6	2057.5	2.7	0.26	0.01	-1021.5	0.83	3.86
Sex + Lat	4	2057.6	2.8	0.25	0.01	-1023.7	0.84	4.05
NDVI + Body mass + avg winter max	5	2057.6	2.8	0.25	0.01	-1022.7	0.86	4.05
NDVI + Sex + Body mass + avg winter max	6	2057.6	2.8	0.25	0.01	-1021.6	0.87	4.05
NDVI + Sex + Body mass + Lat + avg winter min	7	2057.7	2.9	0.24	0.01	-1020.6	0.88	4.26
NDVI + Body mass + Lat + avg winter min	6	2058.1	3.3	0.19	0.01	-1021.8	0.89	5.21
Sex + Lat + avg winter min	5	2058.3	3.5	0.17	0.01	-1023	0.90	5.75
NDVI + Sex + avg summer min	5	2058.3	3.5	0.17	0.01	-1023	0.91	5.75
Sex + Lat + avg summer min	5	2058.4	3.6	0.17	0.01	-1023	0.92	6.06
NDVI + Sex + Body mass + Lat + avg summer max	7	2058.8	4	0.14	0.01	-1021.1	0.92	7.41
NDVI + Sex + Body mass + Lat + avg winter max	7	2059	4.2	0.12	0.01	-1021.2	0.93	8.20
NDVI + Body mass + Lat + avg summer max	6	2059.1	4.3	0.12	0.01	-1022.3	0.93	8.62
Sex + avg winter min	4	2059.2	4.4	0.11	0.01	-1024.5	0.94	9.01
NDVI + Sex	4	2059.2	4.4	0.11	0.01	-1024.5	0.94	9.01
Sex + Lat + avg summer max	5	2059.3	4.5	0.11	0.01	-1023.5	0.95	9.52

NDVI + Body mass + Lat + avg winter max	6	2059.3	4.5	0.11	0.01	-1022.4	0.96	9.52
NDVI + Sex + avg winter min	5	2059.4	4.6	0.1	0.01	-1023.5	0.96	10.00
Sex + Lat + avg winter max	5	2059.6	4.8	0.09	0.01	-1023.6	0.96	10.99
NDVI + Sex + Lat	4	2059.6	4.8	0.09	0.01	-1023.6	0.970	10.99
NDVI + Sex + Lat + avg summer min	6	2059.9	5.1	0.08	0.00	-1022.7	0.97	12.50
Sex	3	2060.3	5.5	0.06	0.00	-1026.1	0.98	15.63
NDVI + Sex + Lat + avg winter min	6	2060.4	5.6	0.06	0.00	-1023	0.98	16.39
Sex + avg summer min	4	2060.5	5.7	0.06	0.00	1025.1	0.98	17.24
NDVI + Sex + avg summer max	5	2061.1	6.3	0.04	0.00	-1024.4	0.98	23.26
NDVI + Sex + avg winter max	5	2061.3	6.5	0.04	0.00	-1024.5	0.99	25.64
NDVI + Sex + Lat + avg summer max	6	2061.4	6.6	0.04	0.00	-1023.5	0.99	27.03
NDVI + Sex + Lat + avg winter max	6	2061.7	6.9	0.03	0.00	-1023.6	0.99	31.25
Sex + avg summer max	4	2062	7.2	0.03	0.00	-1025.9	0.99	37.04
Lat	3	2062.4	7.6	0.02	0.00	-1027.1	0.99	45.46
Sex + avg winter max	4	2062.4	7.6	0.02	0.00	-1026.1	0.99	45.46
NDVI + avg summer min	4	2062.8	8	0.02	0.00	-1026.3	0.99	55.56
Lat + avg winter min	4	2063.1	8.3	0.02	0.00	-1026.5	1.00	62.50
Lat + avg summer min	4	2063.3	8.5	0.01	0.00	-1026.5	1.00	71.43
NDVI	3	2063.7	8.9	0.01	0.00	-1027.8	1.00	83.33
Avg winter min	3	2064	9.2	0.01	0.00	-1027.9	1.00	< 100
NDVI + avg winter min	4	2064	9.2	0.01	0.00	-1026.9	1.00	< 100
Lat + avg summer max	4	2064.2	9.4	0.01	0.00	-1027	1.00	< 100
NDVI + Lat	4	2064.3	9.5	0.01	0.00	-1027	1.00	< 100
Lat + avg winter max	4	2064.4	9.6	0.01	0.00	-1027.1	1.00	< 100
NDVI + Lat + avg summer min	5	2064.6	9.8	0.01	0.00	-1026.1	1.00	< 100
NDVI + Lat + avg winter min	5	2065.1	10.3	0.01	0.00	-1026.4	1.00	< 100
avg summer min	3	2065.3	10.5	0.01	0.00	-1028.6	1.00	< 100
NDVI + avg summer max	4	2065.7	10.9	0.00	0.00	1027.7	1.00	< 100
NDVI + avg winter max	4	2065.8	11	0.00	0.00	-1027.8	1.00	< 100
NDVI + Lat + avg summer max	5	2066.2	11.4	0.00	0.00	-1026.9	1.00	< 100
NDVI + Lat + avg winter max	5	2066.4	11.6	0.00	0.00	-1027	1.00	< 100
avg summer max	3	2066.9	12.1	0.00	0.00	-1029.3	1.00	< 100
avg winter max	3	2067.1	12.3	0.00	0.00	-1029.5	1.00	< 100

(Abbreviations: K=number of model parameters; AICc=Corrected Akaike Information Criterion score, ΔAICc= Change in corrected Akaike Information Criterion score relative to the best fitted model; ModelLik= model likelihood; AICcWt= Corrected Akaike Information Criterion Score weight; LL= log likelihood; Cum.wt= cumulative weight; ER= evidence ratio; Lat= latitude; avg summer max= average summer maximum temperature; avg summer min= average summer minimum temperature; avg winter max= average winter maximum temperature; avg winter min= average winter minimum temperature)

TABLE 3: Summary statistics of the best fit model testing for a relationship between wing area, biological, and environmental variables of *R. capensis* across 9 localities

Variable	Value	SE	DF	t-stat	p-value
Intercept	147.28	11.21	256	13.14	0.00
Average winter maximum temperature	-2.47	1.42	256	-1.74	0.08
Body mass	1.68	0.66	256	2.56	0.01
Sex (Male and Female)	-2.52	1.69	256	-1.49	0.14

(SE= standard error, DF- degrees of freedom; t-stat= t-Statistic)

Body mass was the only significant predictor for differences in wing area. Wing area increases significantly with body mass (Table 3; Figure 2).

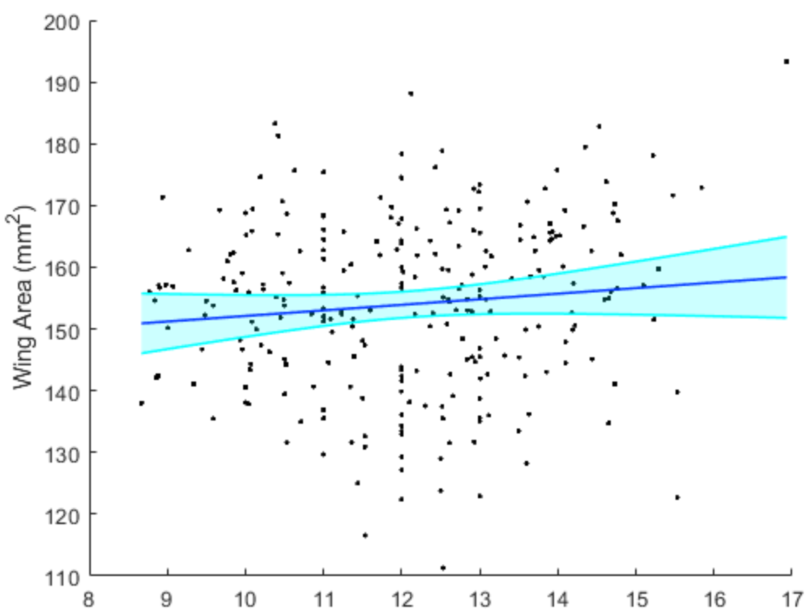

FIGURE 2: Predicted effects of wing area in response to body mass of *R. capensis*. The dark blue line is the trend line. The light blue shading represents a 95 % confidence interval.

There was a statistically significant difference in wing area across localities, ($X^2(8) = 59.017$, $p < 0.00$.) Pairwise comparisons showed significant differences between most of the sites (Table 4). Individuals from Sleepy Hollow, Lekkersing and Zoutpansklipheuwel showed the most significant differences between the other sites. Individuals in Sleepy Hollow were significantly different from the individuals in each other site. Individuals in Lekkersing and Zoutpansklipheuwel were significantly different from those in all sites but two.

The Spearman rank-order correlation determined that there was weak correlation between wing area and each of the biological, environmental, and spatial variables. There was a weak, positive correlation between wing area and body mass, which was not statistically significant (r_s (258) = .102, p = .101). There was a weak, positive correlation between wing area and locality, which was statistically significant (r_s (258) = .154, $p < 0.05$). There was a weak, negative correlation between wing area and sex, which was statistically significant (r_s (258) = -.170, $p < 0.05$). There was a weak, negative correlation between wing area and NDVI, which was statistically significant (r_s (258) = -.233, $p < 0.05$). There was a weak, positive correlation between wing area and latitude, which was statistically significant (r_s (258) = .150, $p < 0.05$). There was a weak, negative correlation between wing area and average winter minimum temperature, which was statistically significant (r_s (258) = -.152, $p < 0.05$). There was a weak, negative correlation between wing area and average winter maximum temperature, which was not statistically significant (r_s (258) = -.018 p = .778). There was a weak, negative correlation between wing area and average summer minimum temperature, which was not statistically significant (r_s (258) = -.004, p = .949). There was a weak, positive correlation between wing area and average summer maximum temperature, which was statistically significant (r_s (258) = -

.063, p = .311). Because there were only weak correlations between the variables, it is reasonable to assume that these variables are not strongly correlated with each other and can thus be included in the same models.

TABLE 4: Pairwise comparison of wing area of *R. capensis* between sample 9 sites in South Africa. P-values are shown in parentheses after the standard error. Significant p-values (< 0.05) are in bold.

Locality	Table Farm	Knysna	Sleepy Hollow	Zoutpansklipheuwel	De Hoop
Table Farm	-	31.85 (0.56)	**18.82 (0.00)**	**15.59 (0.03)**	13.95 (0.93)
Knysna	31.85 (0.56)	-	**35.00 (0.00)**	33.38 (0.11)	32.63 (0.54)
Sleepy Hollow	**18.82 (0.00)**	**35.00 (0.00)**	-	**21.31 (0.00)**	**20.14 (0.00)**
Zoutpansklipheuwel	**15.59 (0.03)**	33.38 (0.11)	**21.31 (0.00)**	-	**17.16 (0.05)**
De Hoop	13.95 (0.93)	32.63 (0.54)	**20.14 (0.00)**	**17.16 (0.05)**	-
Steenkampskral	**18.13 (0.01)**	34.63 (0.50)	**23.23 (0.00)**	**20.67 (0.00)**	**19.49 (0.03)**
Heidehof	18.82 (0.24)	35.00 (0.24)	**23.78 (0.00)**	21.31 (0.56)	20.14 (0.29)
Baviaanskloof	16.76 (0.28)	33.94 (0.99)	**22.19 (0.00)**	**19.51 (0.01)**	18.23 (0.29)
Lekkersing	**29.66 (0.00)**	41.84 (0.11)	**33.02 (0.00)**	**31.29 (0.00)**	**30.51 (0.01)**

Locality	Steenskampskraal	Heidehof	Baviaanskloof	Lekkersing
Table Farm	**18.13 (0.02)**	18.82 (0.24)	16.76 (0.28)	**29.66 (0.00)**
Knysna	34.63 (0.50)	35.00 (0.24)	33.94 (0.99)	41.84 (0.11)
Sleepy Hollow	**23.23 (0.00)**	**23.78 (0.00)**	**22.19 (0.00)**	**33.02 (0.00)**
Zoutpansklipheuwel	**20.70 (0.00)**	21.31 (0.56)	**19.51 (0.01)**	**31.29 (0.00)**
De Hoop	**19.49 (0.03)**	20.14 (0.29)	18.23 (0.29)	**30.51 (0.01)**
Steenkampskraal	-	**23.23 (0.01)**	21.60 (0.27)	32.63 (0.19)
Heidehof	**23.23 (0.01)**	-	22.19 (0.07)	**33.02 (0.00)**
Baviaanskloof	21.60 (0.27)	**22.19 (0.07)**	-	**31.90 (0.04)**
Lekkersing	32.63 (0.18)	**33.02 (0.00)**	**31.90 (0.04)**	-

Prey detection

A total of 175 flight paths from 5 localities (Zoutpansklipheuwel, De Hoop, Lekkersing, Table Farm, and Baviaanskloof) were re-constructed (Figure 3). Lekkersing individuals had the highest calculated prey detection volumes, while Baviaanskloof individuals had the lowest prey detection volumes (Table 1).

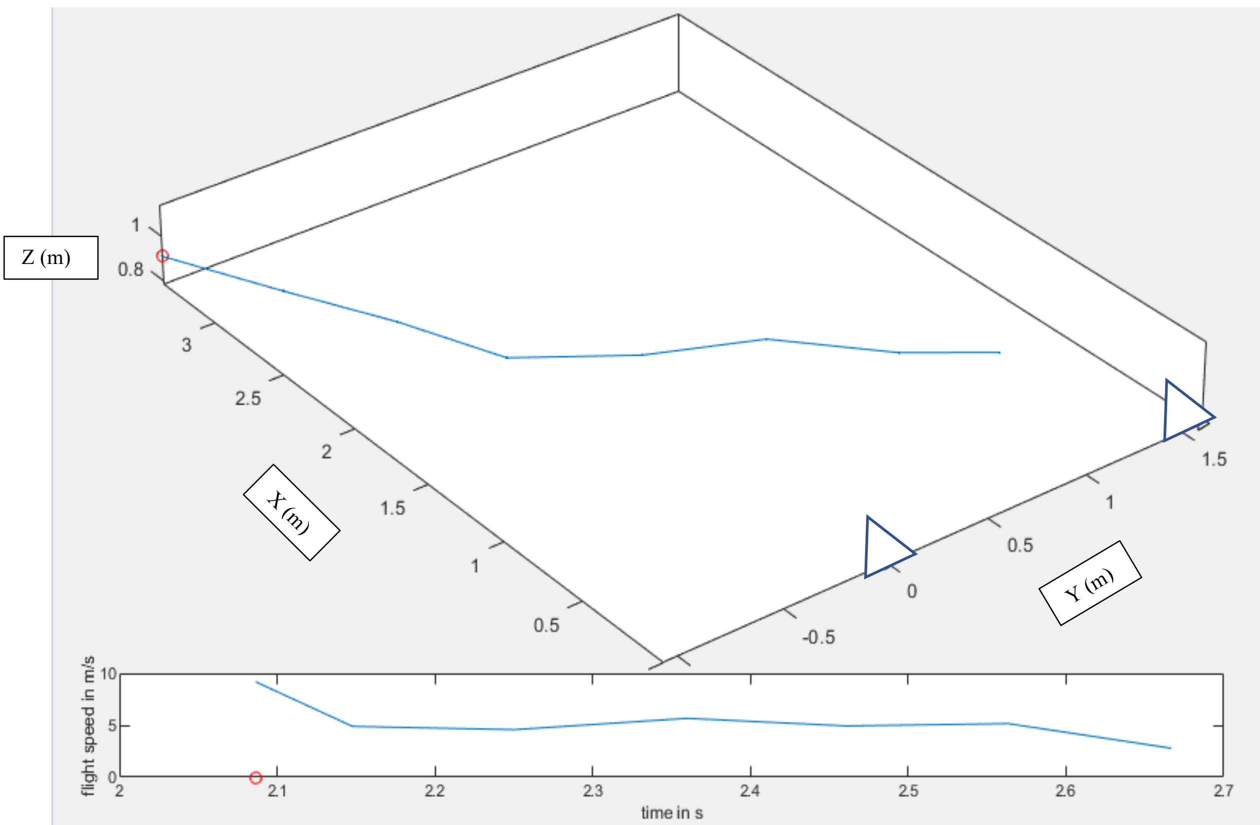

FIGURE 3: Example flight path of *R. capensis* reconstructed from echolocation data. This flight path was generated using a cross-correlation code developed by Holderied and von Helversen (2003) in MATLAB 8.1. The white triangles represent the position of the microphone array system. The blue line represents the reconstructed flight path of the individual bat. The bottom graph shows flight speed (m/s).

The results of the linear mixed effects models were similar for each target strength (-40 dB, -50 dB, and -65 dB). These results showed that the models with the fixed effects of average winter minimum temperature, NDVI, and latitude with the random effect of locality were the best predictors of prey detection volume (Table 5). This model had the lowest AICc value. The top 10 models, which explained more than 94 % of the variability, included NDVI, latitude, and both maximum and minimum temperature (average winter and average summer). Summary statistics revealed that each of these variables was significant (Table 6). There appeared to be deviations in normality of the residuals and high heteroskedasticity (Figures A14, A15 & A16).

TABLE 5: Results of the best fit linear model testing for a relationship between prey detection with environmental and biological variables.

Model	K	AICc	Delta AICc	ModelLik	AICc Wt	LL	Cum. wt	ER
NDVI + Lat + avg winter min	5	1966.7	0	1	0.26	-977.11	0.26	
NDVI + Lat + avg summer min	5	1966.8	0.1	0.951	0.24	-977.13	0.50	1.05
average summer minimum temperature + latitude	4	1968	1.3	0.52	0.13	-978.85	0.63	1.92
Latitude	3	1969.4	2.7	0.26	0.07	-980.57	0.70	3.86
average summer minimum temperature	3	1969.7	3	0.22	0.06	-980.72	0.75	4.48
NDVI + Lat + avg summer max	5	1970	3.3	0.19	0.05	-978.76	0.80	5.21
NDVI + Lat + avg winter max	5	1970	3.3	0.19	0.050	-978.73	0.85	5.21
NDVI + Lat	4	1970.5	3.8	0.15	0.04	-980.06	0.89	6.67
average summer maximum temperature, latitude	4	1971.3	4.6	0.10	0.03	-980.48	0.92	10.00
average winter minimum temperature + latitude	4	1971.4	4.7	0.10	0.024	-980.5	0.94	10.52
NDVI + avg summer min	4	1971.4	4.7	0.01	0.024	-980.53	0.96	10.53
average winter maximum temperature + latitude	4	1971.5	4.8	0.09	0.023	-980.57	0.99	10.99
NDVI + avg summer max	4	1974.3	7.6	0.02	0.01	-981.98	0.99	45.46
NDVI	3	1976.6	9.9	0.01	0.00	-984.2	1.00	> 100
NDVI + avg winter max	4	1976.6	9.9	0.01	0.00	-983.14	1.00	> 100
average summer maximum temperature	3	1977.6	10.9	0.00	0.00	-984.7	1.00	> 100
average winter maximum temperature	3	1977.7	11	0.00	0.00	-984.72	1.00	> 100
average winter minimum temperature	3	1978.1	11.4	0.00	0.00	-984.96	1.00	> 100
NDVI + avg winter min	4	1978.5	11.8	0.00	0.00	-984.07	1.00	> 100

K=number of model parameters; AICc=Corrected Akaike Information Criterion score, ΔAICc= Change in corrected Akaike Information Criterion score relative to the best fitted model; ModelLik= model likelihood; AICcWt= Corrected

Akaike Information Criterion Score weight; LL= log likelihood; Cum.wt= cumulative weight; ER= evidence ratio; Lat= latitude; avg summer max= average summer maximum temperature; avg summer min= average summer minimum temperature; avg winter max= average winter maximum temperature; avg winter min= average winter minimum temperature)

TABLE 6: Summary statistics of the best fit model testing for a relationship between detection volume (TS:-65 dB), biological, and environmental variables. The model including average winter minimum temperature, latitude, and NDVI best explained the variation in prey detection volume of *R. capensis*. All of these variables were significant.

Variable	Value	SE	DF	t-stat	p-value
Intercept	927.76	196.59	171	4.72	0
Average winter minimum temperature	-26.22	10.71	171	-2.45	0.02
Latitude	30.44	7.99	171	3.81	0.00
NDVI	718.04	273.04	171	2.63	0.01

(SE= standard error; DF- degrees of freedom; t-stat= t-Statistic; TS= Target Strength)

Prey detection volume decreased with increasing average winter minimum temperature (Figure 4). Prey detection volume increased with increasing latitude (Figure 5). Latitude is also a predictor that explains the positive effect in prey detection volume (Table 6). Prey detection volume decreases with increasing NDVI scores (Figure 6).

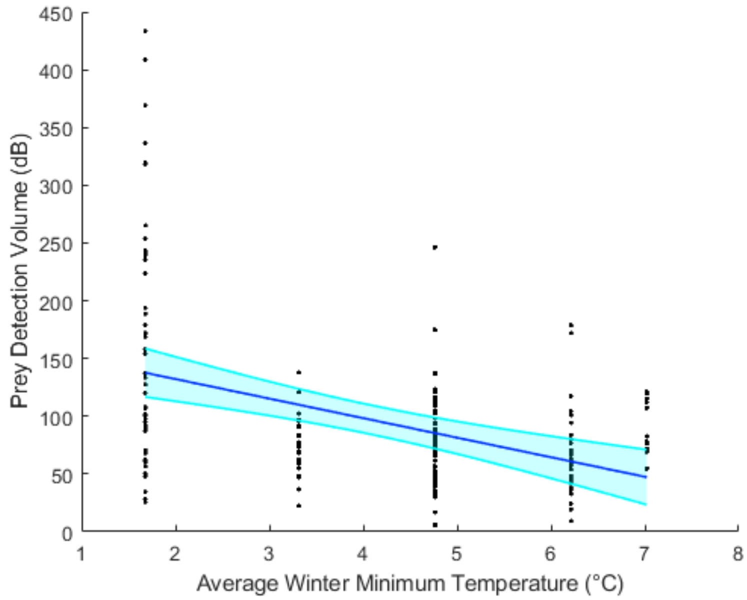

FIGURE 4: Prey detection volume as a function of average winter minimum temperature in *R. capensis***.** The dark blue line is the trend line. The light blue shading represents a 95 % confidence interval.

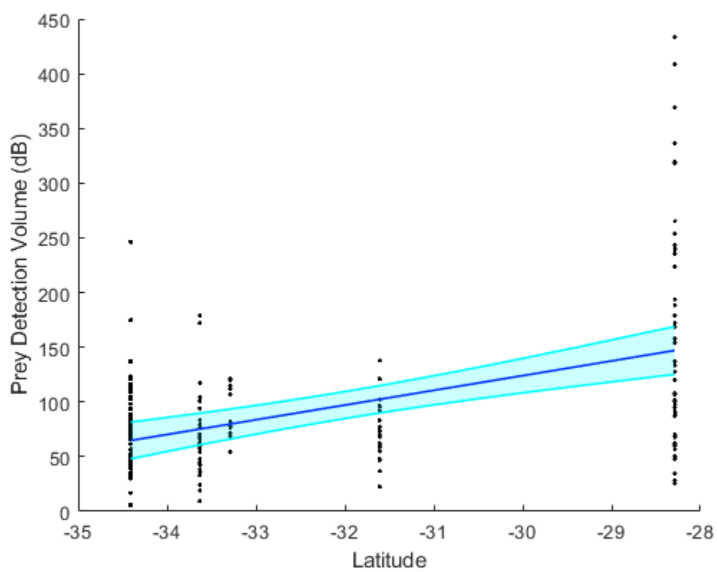

FIGURE 5: Prey detection volume as a function of latitude in *R. capensis*. The dark blue line is the trend line. The light blue shading represents a 95 % confidence interval

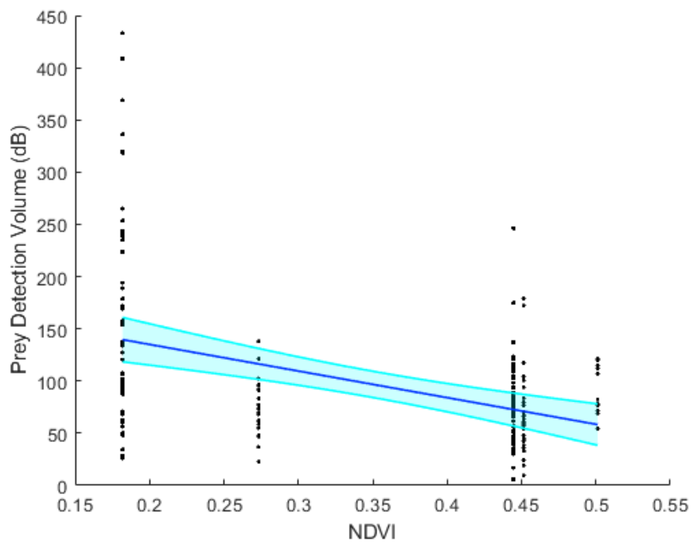

FIGURE 6: Prey detection volume as a function of NDVI in *R. capensis***.** The dark blue line is the trend line. The light blue shading represents a 95 % confidence interval.

A Levene's test revealed there was heterogeneity in the variances for each target strength (-40 dB: X^2 (4) = 21.49, $p < 0.00$; -50 dB: X^2 (4) = 20.94, $p < 0.00$; -65 dB: X^2 (4) = 22.31, $p < 0.00$). A Kolmongrov-Smirnov test did not confirm normality for the residuals at each site for each target strength. I found a significant difference in prey detection volume based on locality (-40 dB: X^2 (4) = 43.60, $p < 0.00$; -50 dB: X^2 (4) =37.46, $p < 0.00$; -65 dB: X^2 (4) = 31.88, $p < 0.00$). Prey detection volume calculated with a target strength of -65 dB showed significant differences between the De Hoop and Lekkersing localities, as well as between the Lekkersing and Baviaanskloof localities ($p < 0.05$) (Table 7). Variation of prey detection volume was greatest within Lekkersing, and it was lowest in Table Farm. Lekkersing had the highest prey detection volumes out of all of the localities, and the average winter minimum temperature was at least 2 degrees lower than the localities where prey detection volume was significantly different.

The Spearman rank-order correlation determined that there was weak correlation between prey detection volume and the environmental and spatial variables. There was a weak, positive correlation between prey detection volume and locality, which was statistically significant (r_s (173) = .204, p < 0.05). There was a weak, positive correlation between prey detection volume and latitude, which was statistically significant (r_s (173) = .342, p < 0.00). There was a weak, negative correlation between prey detection volume and average winter minimum temperature, which was statistically significant (r_s (173) = -.342, p < 0.05). There was a weak, negative correlation between prey detection volume and average winter maximum temperature, which was not statistically significant (r_s (173) = -0.016, p = .836). There was a weak, negative correlation between prey detection volume and average summer minimum temperature, which was statistically significant (r_s (173) = -.361, p < 0.05). There was a weak, positive correlation between prey detection volume and average summer maximum temperature, which was not statistically significant (r_s (173) = -.053, p = .484). There was a weak, negative correlation between prey detection volume and NDVI, which was statistically significant (r_s (173) = -.324, p < 0.05). Because there were only weak correlations between the variables, it is reasonable to assume that these variables are not strongly correlated with each other and can thus be included in the same models.

TABLE 7: Pairwise comparison of prey detection volume of *R. capensis* between sample 5 sites in South Africa. P-values are shown in parentheses after the standard error. Significant p-values (< 0.05) are in bold.

Locality	Kaoo	Lekkersing	De Hoop	Table Farm	Baviaanskloof
Zoutpansklipheuwel	-	**12.72 (0.01)**	12.55 (0.57)	18.57 (0.23)	13.68 (0.13)
Lekkersing	**12.72 (0.0)**	-	**9.81 (0.00)**	16.84 (0.44)	**11.22 (0.00)**
De Hoop	12.55 (0.55)	**9.81 (0.00)**	-	16.71 (0.08)	11.01 (0.21)
Table Farm	18.57 (0.23)	16.84 (0.44)	16.71 (0.08)	-	**17.57 (0.01)**
Baviaanskloof	13.68 (0.13)	**11.22 (0.00)**	11.01 (0.21)	17.57 (0.01)	-

P-values are shown in parentheses after the standard error. Significant p-values (< 0.05) are in bold.

Discussion

Body mass, sex, and average winter minimum temperature were the variables included in the top-fitting model to explain wing size variation. Body mass was the most important indicator of wing area in *R. capensis*. Body mass was included in all of the top fitting models, and it was the only significant predictor of wing area in the top fitting model. Although the variables sex and average winter minimum temperature were in the best model explaining wing area, they were not significant, meaning these variables only contribute to changes in wing area when combined with body mass.

Body mass was the only significant determinant of wing area, which was inconsistent with my prediction that environmental variables would have a relationship with wing area. This is likely due to the positive relationship between wing loading and body mass. Larger wings are needed to support larger bodies and generate sufficient lift for flight (Norberg, 1981). Bats sampled from Lekkersing had the largest average wing areas, and bats sampled from Sleepy Hollow had the smallest average wing areas. Based on the raw data, this relationship was also true of their body masses. Wing area variation is likely best explained by body mass with allometric responses in wing area, since both average winter minimum temperature and sex influence wing area, but only when combined with body mass. The relationship between body mass and wing area is supported by literature on rhinolophids in southern Africa. For example, Jacobs and Bastian (2018) suggest that there is selective pressure to maintain the allometric relationship between body mass and wing loading (which would consequently affect wing area) due to rhinolophid's specialization of foraging in highly-cluttered areas. HDC echolocators must have low wing loading in order to effectively utilize the HDC system of echolocation which allows them to maneuver close to vegetation so that emitted pulse and echo overlap, enabling determination by the flying bat of the degree doppler shift compensation required (Schuller, 1974). Therefore, the selective pressures that may result from sexual selection and temperature are constrained due to the adaptive complex formed by echolocation and wings of rhinolophids (Jacobs and Bastian, 2018)

That sex did not explain any of the variation in wing area is not uncommon in rhinolophids. While there was slight variation in wing area between males and females, with females being slightly larger, this variable was not significant. This trend is consistent with a study by Wu et al. (2018) which showed slight female-biased sexual size dimorphism in *R. capensis*, but no support for sexual size dimorphism in horseshoe bats overall. This is likely due to the weak selective pressure on larger body size in males, and the strong selective pressure for larger body size in females (Wu et al., 2018). Mutumi et al., (2016) also found no sexual dimorphism in the size of rhinolophid bats, and Jacobs and Bastian (2018) found no differences in the wingspan and body mass of *R. capensis* between the sexes. Jacobs & Bastian (2018) attributed the lack of sexual dimorphism in *R. capensis* to a variety of selection pressures and genetic drift that constrain the evolution of sexual dimorphism in rhinolophids. The inclusion of sex in the top fitting model is likely due to the fact that it is only significant when combined with body mass.

Contrary to my prediction, average winter minimum temperature was not a significant predictor of wing area, despite its inclusion in the top fitting model. Wing areas were slightly larger in climates with lower average winter minimum temperature, but this is likely due to these bats also having larger body masses in these regions. The combination of behavioral mechanisms and other morphological components that bats have to assist in thermoregulation likely make the effect of temperature on wing area negligible. For example, many rhinolophids use evaporative water loss for cooling by panting and licking the bodies (Lyman P., 1970). At low temperatures, blood flow to their extremities is reduced, and colony members will huddle together to increase heat exchange (Lyman, 1970). Entry into torpor is also directly affected by ambient air temperature in *R. capensis* (Brown and Bernard, 1994). Torpor is a state of a decreased body temperature, allowing bats to reduce their physiological activity and metabolic rate (Wang, 1989). Brown and Bernard (1994) documented the need for *R. capensis* to find a roost that is sufficiently cold in the winter to induce hibernation or torpor while being hot enough in the summer to lower the metabolic costs of thermoregulation. *Rhinolophus capensis* also frequently changes positions within roosts to meet their thermal preferences. It is likely that any combination of these behavioral mechanisms for thermoregulation play a much larger role in maintaining the stable body temperatures of *R. capensis* than the effect that larger wings would have. It is also possible that the need for efficient flight outweighs the thermoregulatory benefit that increases in wing area would provide.

Although there was no significant relationship between temperature and wing area, a relationship could exist between body size and temperature. For example, James' rule suggests that the body size of a species will be smallest in a hot, humid environment, slightly larger in cool, humid environments and largest in a cool, dry environment (James, 1970). Having a larger body allows for greater heat conservation because of the lower surface area to volume ratio (Bergmann, 1847; Meiri and Dayan, 2003). This relationship has been observed in bats, with smaller bats experiencing greater fluctuations in body heat than larger bats over a similar ambient temperature range (Thomas et al., 1991). Selection for different body sizes has led to the speciation of rhinolophids across southern Africa, resulting in allometric responses in echolocation too (Stoffberg et al., 2011; Taylor et al., 2012). Wang et al. (2020) also suggested possible adaptation for heat conservation in colder environments due to the correlations between body size and average winter minimum temperature. It is possible that average winter minimum temperature may be better correlated with body size in *R. capensis* too, given this variable's inclusion in the top fitting model. *R. capensis* was heaviest in the environment (desert) with the lowest average winter minimum temperature; the temperature that bats are likely to experience when active at night. The desert also had the highest average summer maximum temperature (Lekkersing) but roosting bats probably deal with such conditions behaviorally by roosting in cool dark caves which are buffered against the high diurnal temperatures (Kunz and Fenton, 2003; Twente, 1955). The possible correlations between body size and temperature in *R. capensis* (i.e. James' rule) should be explored in future studies.

While the relationship between wing area and body mass is supported, it is interesting that NDVI was not a significant variable in the best fitting model (Norberg and Rayner, 1987). Larger wings relative to body mass decrease wing loading and increase maneuverability in flight (Norberg and Rayner, 1987), and bats with higher wing loading tend to forage in areas with less vegetation, where maneuverability is likely not as crucial to foraging success (Aldridge and Rautenbach, 1987). I would have expected to see NDVI as a significant determinant of wing area, with larger relative wing areas in less cluttered environments, and smaller relative wing areas in more cluttered environments. The reasons behind the lack of support could be due to a possible correlation between NDVI and wing loading, and not NDVI and wing area, since wing loading is driven by both body size and wing area. The relationship between wing area and body mass is not linear, with wing area increasing at a slower rate in proportion to body mass (Jones, 1996). However, because I focused on climactic effects, wing area rather than wing loading was used in my models. Furthermore, both wing loading and body mass could not be considered together given the collinearity between the variables (Norberg and Rayner, 1987). Senawi and Kingston (2019) also showed that body mass and wing loading were the only significant predictors of maneuverability in highly cluttered environments. This is a consistent trend, with wing loading accounting for differences in maneuverability in many species, including *Rhinolophus ferrumequinum*, *Rhoniscus papuensis*, and *Hipposideros ruber* (Aldridge, 1987; Jones et al., 1993; Rhodes, 1995) It is also possible that seasonal NDVI values, versus the long-term averages, would be better related to wing area.

The low proportion of variation explained by the top fitting models suggests that other variables I did not consider likely have a larger impact on wing area. For example, prey size is positively related to body size (Black, 1974; McNab, 1969), which could in turn, affect the evolution of wing area. This trend has been observed in other rhinolophid bats, where larger bats tend to eat prey of various sizes, where small bats are limited to smaller prey items (Andreas et al., 2013). Jacobs et al. (2007) reported evidence that supported this trend while studying the diets of *R. capensis* and *R. clivosus* living in the same environment. While the contents of their diets overlapped, the prey items captured by *R. capensis* were significantly smaller than those captured by *R. clivosus* (Jacobs et al., 2007). *R. clivosus* is significantly larger than *R. capensis* in body size and wing area.

The models for prey detection volume revealed that NDVI, latitude, and average winter minimum temperature were the best predictors of prey detection volume. All of these variables explained variation in prey detection volume. Latitude explained most of the variation in prey detection volume, followed by NDVI and average winter minimum temperature. It is likely that these variables all select for detection volume concurrently, given that they were all significant in the top-fitting model. The relationship I found between latitude and prey detection volume was predictable. Geographic variation in echolocation pulse design is common for rhinolophids, and has been studied widely in species including *R. pusillus, R. ferrumequinum, R. clivosus, and R. damarensis*, a species closely related to *R. capensis*. (Jacobs et al., 2017; Jiang et al., 2015; Maluleke et al., 2017; Sun et al., 2013). Studies on *R. capensis* confirm that its peak echolocation frequency (the frequency of its CF component) varies across its range, with the lowest frequency of 75 kHz in the northwest part of its range (in the desert), increasing to a maximum of 86 kHz in the more forested southeastern part of its range (Odendaal et al., 2014). This increase in echolocation frequency with latitude is probably associated with the increase in the amount of vegetation from the desert in the northwest to the forests and fynbos of the forests in the southwest. This is supported by the similar trend in NDVI which is a proxy for the degree of clutter in the different habitats occupied by *R. capensis*. For example, the northwest portion of its range has an average NDVI value of 0.18 in Lekkersing, while the southeast portion of its range has an average NDVI value of 0.80 in Knysna. These sites are separated by over 5 degrees, with Lekkersing at latitude -28.29 and Knysna at latitude -34.08. Odendaal et al. (2014) suggested that the individual variation in *R. capensis* across its range is due to the local adaptation of echolocation call frequencies to lower frequency calls in less-cluttered environments. My data are consistent with the results of Odendaal et al. (2014), showing decreased prey detection volumes in environments with higher NDVI values. Lower frequency pulses are less affected by atmospheric attenuation than high frequency pulses (Lawrence and Simmons, 1982). In an environment with low amounts of environmental clutter, it is more beneficial for a HDC echolocating bat to use low frequency pulses to increase detection distance (Jakobsen et al., 2013; Jones and Holderied, 2007). Increasing the detection distance of a pulse is necessary to find prey in more open spaces, as bats have larger volumes of space to search in which prey density is lower. In contrast, higher frequency pulses provide greater directionality over the shorter distances in more cluttered space, thereby increasing the bat's chances of successfully finding and capturing prey in more cluttered environments (Neuweiler et al., 1987; Rydell et al., 1995). Although higher frequency pulses are more affected by atmospheric attenuation, detection distance is not as crucial when foraging in highly cluttered environments. Therefore, it is unsurprising to see both NDVI and latitude as significant variables in the top-fitting model for prey detection volume.

Average winter minimum temperature was also significantly correlated with prey detection volume, a trend consistent with initial prediction arising from the hypothesis. Prey detection volume decreased with increasing average winter minimum temperature. In other words, the highest prey detection volumes were recorded in environments with the lowest winter minimum temperatures. This is not surprising, given that warmer environments attenuate pulses more rapidly (Attenborough, 2008). Data for other species of rhinolophids in southern Africa are similar, also showing correlation between echolocation pulse design and temperature (Maluleke et al., 2017; Mutumi et al., 2016). However, other studies on *R. capensis* reported no relationship between air temperature and resting frequency at all (e.g. Odendaal et al., 2014; Stoffberg, 2007). It is likely that temperature and other environmental variables, like humidity and rainfall, determines the prey detection volume of *R. capensis* due to the interaction of all of these components in determining atmospheric attenuation. Furthermore, the low explanatory value of temperature is likely due to the fact that *R. capensis* is a hibernating bat that likely does not regularly experience cold winter temperatures when foraging (Bernard, 1985).

One such variable that likely influences echolocation in conjunction with temperature is humidity. In horseshoe bats, humidity plays a significant role in determining call design (Jiang et al., 2015; Maluleke et al., 2017; Mutumi et al., 2016). Other studies show that bats actively lower the frequency of the pulses in response to humid conditions (e.g. Chaverri and Quirós, 2017; Guillén et al., 2000) since highly humid conditions more rapidly absorb sound due to atmospheric attenuation. Because *R. capensis* occupies a wide range with climactic variations in humidity, these trends are especially important. Maluleke et al. (2017) found that in arid regions, temperature alone plays a significant role in determining call design. However, Jacobs et al. (2017) showed that *Rhinolophus clivosus* in both arid and temperate will be influenced by temperature in the arid regions, and humidity in the temperate regions. The nonlinear relationship between temperature and humidity could explain why Odendaal and Jacobs (2011) found no correlation between humidity and resting frequency in *R. capensis*. That is, the authors argue that no relationship between these two variables exist because temperature and humidity interact concurrently to influence pulse design. It is important that future studies examine the interaction between humidity and temperature and the potential influence of temperature and humidity on the detection volume of bats existing across varying ecosystems. Rainfall could also potentially impact the resting frequency, and therefore the detection distance, of echolocation pulses (Guillén et al., 2000; Jiang et al., 2015). Based on the highly varying rainfall across the range of *R. capensis*, it is likely that this variable may too have an influence on its prey detection volume (Hersbach et al., 2020; Lobelia, 2020). This study did not explore the potential impacts of humidity and rainfall on the prey detection volume of *R. capensis* due to the complex interactions between these variables and the limited scope of my question.

Prey detection volume is influenced by both detection distance and beam width (Luo et al., 2014). Since I used the same beam width across all localities, differences in prey detection volume are likely due to changes in detection distance. However, it is unlikely that all *R.*

capensis use the same beam widths when foraging as bats can actively adjust the widths of their sonar beams. (Jakobsen and Surlykke, 2010; Matsuta et al., 2013; Surlykke et al., 2009). While difficult to measure, having more precise measurements of a bat's beam width while foraging can provide more accurate estimations for the true directionality and intensity of the sonar beam. In the search phase, beam widths are typically narrower, increasing the detection distance, directionality, and intensity of the pulse (Jakobsen and Surlykke, 2010; Matsuta et al., 2013). In the terminal phase, bats broaden the beam to ensure that the moving target remains within the cone of detection (Jakobsen et al., 2013; Matsuta et al., 2013). Individuals within the same populations likely change their beam width depending on whether they are in the search or terminal phase. Furthermore, because *R. capensis* forages across a wide range of ecoregions with varying amounts of environmental clutter, it is likely that different populations use different beam widths in different situations. While it may only be possible in highly-controlled conditions, future studies should attempt to quantify the beam widths of *R. capensis* to give better insight into the flexibility of pulses of HDC echolocators.

The avoidance of interspecific competition may also influence the prey detection volumes of *R. capensis*. *Rhinolophus capensis* overlaps in range with various other species, including *Rhinolophus damerensis, Rhinolophus clivosus,* and *Miniopterus natalensis* (Jacobs et al., 2007). Differences in echolocation call frequency in *R. capensis* may have been selected for as a means of competition avoidance. Variation in frequency of echolocation calls affects the target detection of prey items of varying size, with higher frequency calls better able to detect flying insects (Jones et al., 1992). Higher frequency calls also increase the detection distance. Fawcett et al. (2015) found that *R. capensis* alters its calls when flying with other bat species. When flying with *Miniopterus natalensis,* the calls of *R. capensis* had a longer FM component and lower minimum frequencies. When flying with *Rhinilophus clivosus,* a larger HDC echolocating bat, *R. capensis* made calls of a shorter duration. Differences in body size may have resulted from changes in echolocation frequencies. Notably, *R. damerensis* and *R. cliovosus* are larger than *R. capensis*, and both species echolocate at lower frequencies. Differences in echolocation frequency may be coupled with other morphological characteristics, like nasal chamber length and body size (Robinson, 1996). Odendaal and Jacobs (2011) found that and nasal chamber length was correlated with resting frequency in *R. capensis,* supporting this idea. Since *R. capensis* echolocates at different resting frequencies across its range, the possibility of competition avoidance affecting prey detection volumes in *R. capensis* should be explored by examining differences in diet in populations of *R. capensis* across its range and between interspecific populations.

The inclusion of average winter minimum temperature in the top-fitting models for both wing area and prey detection volume suggest that both of these attributes are influenced by environmental conditions and will thus be affected by environmental changes. For example, if body size in *R. capensis* follow Bergmann's rule, then selection for changes in body size due to increases in ambient temperature will likely lead to changes in wing area as well. Changes in wing area can affect flight performance if wing loading does not properly account for the amount of environmental clutter. Additionally, increases in ambient temperature may also directly affect the prey detection ability of echolocating bats, since warmer environments more readily absorb sound. The average winter minimum temperature is 1.67 °C in Lekkersing, 4.76 °C in De Hoop, and 6.21 °C in Baviaanskloof. As the average winter minimum temperatures in Lekkersing, De Hoop, and Baviaanskloof differed by more than 2 °C, and was a significant variable in the top-fitting model, it is likely that climate change would lead to a reduced prey detection volume of *R.*

capensis, similar to the trends described by (Luo et al., 2014). Climate change can also affect other biotic factors, such as insect abundance, that *R. capensis* relies on for survival (Jones et al., 2009). This would have a direct impact on various factors, including the echolocation efficacy of *R. capensis*.

Increases in ambient temperature may also have some indirect effects on the foraging efficiency of echolocating bats. For example, temperature impacts both the amount and type of vegetation. Various projections predict changes in both the amount of vegetation and vegetation type as a result of climate change in southern Africa (Bond et al., 2003; Buitenwerf et al., 2012; Scheiter and Higgins, 2009; Wilson et al., 2015). Notably, Scheiter and Higgins (2009) predicted that higher atmospheric temperature and increases in CO_2 would lead to major shifts towards tree-dominated ecosystems and increases in biomass, with grassland ecosystems changing to savanna ecosystems and savanna ecosystems changing to deciduous woodland ecosystems. As NDVI significantly determined differences in prey detection volume, changes in vegetation abundance and structure would likely lead to changes in prey detection volume as well. It is also important that future studies examine the relationship between wing loading and NDVI in *R. capensis*, as wing shape has also been shown to be correlated with environmental clutter (Aldridge and Rautenbach, 1987; Norberg and Rayner, 1987).

The results of this study provide evidence that the wing area and prey detection volume of *R. capensis* is adapted to local climactic conditions. These results therefore provide important evidence that the foraging efficiency of rhinolophid bats is dependent on environmental conditions, including ambient temperature and clutter, and that changes to the environment will select for adaptive change in these animals reliant on acoustic signals. Although bat wings do not likely function primarily as a thermoregulatory appendage, changes in ambient temperature are still likely to affect wing area due to allometric changes in body size, therefore affecting the foraging efficiency of bats (Jacobs and Bastian, 2018). Furthermore, the HDC echolocation of *R. capensis* is likely to be affected due to decreases in prey detection volume from increased atmospheric attenuation. The adaptive complex between these traits also pose a risk to *R. capensis*, because changes in one of these traits is likely to affect the other as well (Aldridge and Rautenbach, 1987; Jacobs and Bastian, 2018; Norberg and Rayner, 1987). Decreases in the foraging efficiency of *R. capensis* make them vulnerable to the effects of human-induced climate change because of the rapidity of such changes (Luo et al., 2014; Sherwin et al., 2013). If bats are unable to adapt to local climactic conditions, this could lead to local extinction and losses of the ecosystem services bats provide. Climate induced variation in the morphically and sensory adaptations of bat species must continue to be studied, specifically focusing on the complex interactions that exist between environmental variables, and by looking at alternative variables that may capture more variability. Furthermore, climate change's impact on overall landscape change should be studied because of the observed relationships between environmental clutter and echolocation call design. Only such studies will aid our understanding of how rapid human-induced climate change is likely to impact ecosystems.

References

Adams, R.A., 2010. Bat reproduction declines when conditions mimic climate change projections for western North America. Ecology 91, 2437–2445. https://doi.org/10.1890/09-0091.1

Akaike, H., 1998. Information Theory and an extension of the maximum likelihood principle. pp. 199–213. https://doi.org/10.1007/978-1-4612-1694-0_15

Aldridge, H.D.J.N., 1987. Turning flight of bats. J. Exp. Biol. 128, 419–425.

Aldridge, H.D.J.N., Rautenbach, I.L., 1987. Morphology, echolocation and resource partitioning in insectivorous bats. J. Anim. Ecol. 56, 763–778. https://doi.org/10.2307/4947

Andreas, M., Reiter, A., Cepáková, E., Uhrin, M., 2013. Body size as an important factor determining trophic niche partitioning in three syntopic rhinolophid bat species. Biol. 68, 170–175. https://doi.org/10.2478/s11756-012-0139-1

Anthony, E., 1998. Age determination in bats, in: Ecological and behavioral methods for the study of bats. pp. 47–58. Smithsonian Institute Press, Washington, DC

Anthony, E.L.P., Stack, M.H., Kunz, T.H., 1981. Night roosting and the nocturnal time budget of the little brown bat, *Myotis lucifugus*: Effects of reproductive status, prey density, and environmental conditions. Oecologia 51, 151–156. https://doi.org/10.1007/BF00540593

Araújo, M.B., Ferri-Yáñez, F., Bozinovic, F., Marquet, P.A., Valladares, F., Chown, S.L., 2013. Heat freezes niche evolution. Ecol. Lett. 16, 1206-1219. https://doi.org/10.1111/ele.12155

Arita, H.T., Fenton, M.B., 1997. Flight and echolocation in the ecology and evolution of bats. Trends Ecol. Evol. 12, 53-58. https://doi.org/10.1016/S0169-5347(96)10058-6

Attenborough, K., 2008. Sound propagation in the atmosphere, in: Handbook of Noise and Vibration Control. pp. 67–78. Springer, New York, NY.

https://doi.org/10.1002/9780470209707.ch5

Avery, M.I., 1985. Winter Activity of Pipistrelle Bats. J. Anim. Ecol. 54, 721-738. https://doi.org/10.2307/4374

Avila-Flores, R., Medellín, R.A., 2004. Ecological, taxonomic, and physiological correlates of cave use by Mexican bats. J. Mammal. 85, 675–687. https://doi.org/10.1644/bos-127

Barclay, R.M.R., 1991. Population structure of temperate zone insectivorous bats in relation to foraging behaviour and energy demand. J. Anim. Ecol. 60, 165–178. https://doi.org/10.2307/5452

Bartholomew, G.A., Leitner, P., Nelson, J.E., 1964. Body temperature, oxygen consumption, and heart rate in three species of Australian flying foxes. Physiol. Zool. 37, 179–198. https://doi.org/10.1086/physzool.37.2.30152330

Bastian, A., Jacobs, D.S., 2015. Listening carefully: Increased perceptual acuity for species discrimination in multispecies signalling assemblages. Anim. Behav. 101, 141–154. https://doi.org/10.1016/j.anbehav.2014.12.010

Bell, G.P., Fenton, M.B., 1984. The use of Doppler-shifted echoes as a flutter detection and clutter rejection system: the echolocation and feeding behavior of *Hipposideros ruber* (Chiroptera: Hipposideridae). Behav. Ecol. Sociobiol. 15, 109–114. https://doi.org/10.1007/BF00299377

Bergmann, C., 1847. Über die verhältnisse der wärmeökonomie der thiere zu ihrer grösse, göttinger studien. *Gottinger studien,* v. 3, pt. 1, pp. 595-708.

Bernard, R.T.F., 1985. Reproduction in the Cape horseshoe bat (*Rhinolophus capensis*) from South Africa. South African J. Zool. 20, 129–135. https://doi.org/10.1080/02541858.1985.11447925

Black, H.L., 1974. A north temperate bat community: Structure and prey populations. J. Mammal. 55, 138–157. https://doi.org/10.2307/1379263

Bond, W.J., Midgley, G.F., Woodward, F.I., 2003. What controls South African vegetation - Climate or fire? South African J. Bot. 69, 79–91. https://doi.org/10.1016/S0254-6299(15)30362-8

Boonman, A., Ostwald, J., 2007. A modeling approach to explain pulse design in bats. Biol. Cybern. 97, 159–172. https://doi.org/10.1007/s00422-007-0164-2

Brinkløv, S., Kalko, E.K.V., Surlykke, A., 2010. Dynamic adjustment of biosonar intensity to habitat clutter in the bat *Macrophyllum macrophyllum* (Phyllostomidae). Behav. Ecol. Sociobiol. 64, 1867–1874. https://doi.org/10.1007/s00265-010-0998-9

Bronner, G.N., Maloney, S.K., Buffenstein, R., 1999. Survival tactics within thermally-challenging roosts: Heat tolerance and cold sensitivity in the Angolan free-tailed bat, *Mops condylurus*. South African J. Zool. 34, 1–10. https://doi.org/10.1080/02541858.1999.11448481

Brown, C.R., Bernard, R.T.F., 1994. Thermal preference of Schreiber's long-fingered (*Miniopterus schreiberisii*) and Cape horseshoe (*Rhinolophus capensis*) bats. Comp. Biochem. Physiol. Part A Physiol. 107, 439–449. https://doi.org/10.1016/0300-9629(94)90023-X

Buitenwerf, R., Bond, W.J., Stevens, N., Trollope, W.S.W., 2012. Increased tree densities in South African savannas: >50 years of data suggests CO_2 as a driver. Glob. Chang. Biol. 18, 675–684. https://doi.org/10.1111/j.1365-2486.2011.02561.x

Chaverri, G., Quirós, O.E., 2017. Variation in echolocation call frequencies in two species of free-tailed bats according to temperature and humidity. J. Acoust. Soc. Am. 142, 146–150.

https://doi.org/10.1121/1.4992029

Cleveland, C.J., Betke, M., Federico, P., Frank, J.D., Hallam, T.G., Horn, J., Kunz, T.H., Lopez Jr., J.D., McCracken, G.F., Medellín, R.A., Moreno-Valdez, A., Sasone, C.G., Westbrook, 2006. Estimation of the economic value of the pest control service provided by the Brazilian Free-tailed bat in the winter garden region of south-central Texas. Front. Ecol. Environ. 4, 238-243. https://doi.org/10.1890/15409295(2006)004[0238:EVOTPC]2.0.CO;2

Denzinger, A., Schnitzler, H.U., 2013. Bat guilds, a concept to classify the highly diverse foraging and echolocation behaviors of microchiropteran bats. Front. Physiol. 4 July, 1–15. https://doi.org/10.3389/fphys.2013.00164

Didan, K., 2015. MOD13Q1 MODIS/Terra Vegetation Indices 16-Day L3 Global 250m SIN Grid V006. https://doi.org/https://doi.org/10.5067/MODIS/MOD13Q1.006

Dinerstein, E., Olson, D., Joshi, A., Vynne, C., Burgess, N.D., Wikramanayake, E., Hahn, N., Palminteri, S., Hedao, P., Noss, R., Hansen, M., Locke, H., Ellis, E.C., Jones, B., Barber, C.V., Hayes, R., Kormos, C., Martin, V., Crist, E., Sechrest, W., Price, L., Baillie, J.E.M., Weeden, D., Suckling, K., Davis, C., Sizer, N., Moore, R., Thau, D., Birch, T., Potapov, P., Turubanova, S., Tyukavina, A., De Souza, N., Pintea, L., Brito, J.C., Llewellyn, O.A., Miller, A.G., Patzelt, A., Ghazanfar, S.A., Timberlake, J., Klöser, H., Shennan-Farpón, Y., Kindt, R., Lillesø, J.P.B., Van Breugel, P., Graudal, L., Voge, M., Al-Shammari, K.F., Saleem, M., 2017. An ecoregion-based approach to protecting half the terrestrial realm. Bioscience. https://doi.org/10.1093/biosci/bix014

Dool, S.E., Puechmaille, S.J., Foley, N.M., Allegrini, B., Bastian, A., Mutumi, G.L., Maluleke, T.G., Odendaal, L.J., Teeling, E.C., Jacobs, D.S., 2016. Nuclear introns outperform mitochondrial DNA in inter-specific phylogenetic reconstruction: Lessons from horseshoe bats (Rhinolophidae: Chiroptera). Mol. Phylogenet. Evol. 97, 196–212. https://doi.org/10.1016/j.ympev.2016.01.003

Erickson, J.L., West, S.D., 2002. The influence of regional climate and nightly weather conditions on activity patterns of insectivorous bats. Acta Chiropterologica 4, 17–24. https://doi.org/10.3161/001.004.0103

Falk, B., Jakobsen, L., Surlykke, A., Moss, C.F., 2014. Bats coordinate sonar and flight behavior as they forage in open and cluttered environments. J. Exp. Biol. 217, 4356–4364. https://doi.org/10.1242/jeb.114132

Fawcett, K., Jacobs, D.S., Surlykke, A., Ratcliffe, J.M., 2015. Echolocation in the bat, *Rhinolophus capensis*: The influence of clutter, conspecifics and prey on call design and intensity. Biol. Open 4, 693–701. https://doi.org/10.1242/bio.201511908

Fenton, M.B., 1999. Describing the echolocation calls and behaviour of bats. Acta Chiropterologica 1, 127–136.

Fenton, M.B., 1995. Natural history and biosonar signals. In: Popper A.N., Fay R.R. (eds) Hearing by Bats. Springer Handbook of Auditory Research, vol 5. Springer, New York, NY. pp. 37–86. https://doi.org/10.1007/978-1-4612-2556-0_2

Fenton, M.B., 1990. The foraging behaviour and ecology of animal-eating bats. Can. J. Zool. 68, 411–422. https://doi.org/10.1139/z90-061

Fenton, M.B., Faure, P.A., Ratcliffe, J.M., 2012. Evolution of high duty cycle echolocation in bats. J. Exp. Biol. 215, 2935–2944. https://doi.org/10.1242/jeb.073171

Flory, A.R., Kumar, S., Stohlgren, T.J., Cryan, P.M., 2012. Environmental conditions associated with bat white-nose syndrome mortality in the north-eastern United States. J. Appl. Ecol. 49, 680–689. https://doi.org/10.1111/j.1365-2664.2012.02129.x

Griffin, D.R., 1958. Listening in the dark: the acoustic orientation of bats and men. Yale University Press, New Haven, CT.

Guillén, A., Juste B, J., Ibáñez, C., 2000. Variation in the frequency of the echolocation calls of *Hipposideros ruber* in the Gulf of Guinea: An exploration of the adaptive meaning of the constant frequency value in rhinolophoid CF bats. J. Evol. Biol. 13, 70–80. https://doi.org/10.1046/j.1420-9101.2000.00155.x

Hall, L.S., 1982. The effect of cave microclimate on winter roosting behaviour in the bat, *Miniopterus schreibersii blepotis*. Aust. J. Ecol. 7, 129–136. https://doi.org/10.1111/j.1442-9993.1982.tb01586.x

Henson, O.W., 1965. The activity and function of the middle-ear muscles in echo-locating bats. J. Physiol. 180, 871–887. https://doi.org/10.1113/jphysiol.1965.sp007737

Hersbach, H., Bell, B., Berrisford, P., Hirahara, S., Horányi, A., Muñoz-Sabater, J., Nicolas, J., Peubey, C., Radu, R., Schepers, D., Simmons, A., Soci, C., Abdalla, S., Abellan, X., Balsamo, G., Bechtold, P., Biavati, G., Bidlot, J., Bonavita, M., De Chiara, G., Dahlgren, P., Dee, D., Diamantakis, M., Dragani, R., Flemming, J., Forbes, R., Fuentes, M., Geer, A., Haimberger, L., Healy, S., Hogan, R.J., Hólm, E., Janisková, M., Keeley, S., Laloyaux, P., Lopez, P., Lupu, C., Radnoti, G., de Rosnay, P., Rozum, I., Vamborg, F., Villaume, S., Thépaut, J.N., 2020. The ERA5 global reanalysis. Q. J. R. Meteorol. Soc. 146, 1999–2049. https://doi.org/10.1002/qj.3803

Hoare, D.B., Mucina, L., Rutherford, M.C., Volk, J.H.J., Euston-Brown, D.I.W., Palmer, A.R., Powrie, L.W., Lechmere-Oertel, R.G., Proches, S.M., Dold, A.P., Ward, R.A., 2006. Albany Thicket Biome. Veg. South Africa, Lesotho Swazil. 541–567.

Holderied, M.W., Korine, C., Fenton, M.B., Parsons, S., Robson, S., Jones, G., 2005.

Echolocation call intensity in the aerial hawking bat *Eptesicus bottae* (Vespertilionidae) studied using stereo videogrammetry. J. Exp. Biol. 208, 1321–1327. https://doi.org/10.1242/jeb.01528

Holderied, M.W., Von Helversen, O., 2003. Echolocation range and wingbeat period match in aerial-hawking bats. Proc. R. Soc. B Biol. Sci. 270, 2293–2299. https://doi.org/10.1098/rspb.2003.2487

Ibáñez, C., 1997. Winter reproduction in the greater mouse-eared bat (*Myotis myotis*) in South Iberia. J. Zool. 243, 836–840. https://doi.org/10.1111/j.1469-7998.1997.tb01981.x

IPCC, 2018. An IPCC Special Report on the impacts of global warming of 1.5°C. Intergov. Panel Clim. Chang. https://doi.org/10.1002/9780470996621.ch50

ISO, 1996. Acoustics - Attenuation of sound during propagation outdoors -- Part 1: Calculation of the absorption of sound by the atmosphere, Iso 9613-1:1993. Geneva.

Jacobs, D.S., Barclay, R.M.R., Walker, M.H., 2007. The allometry of echolocation call frequencies of insectivorous bats: Why do some species deviate from the pattern? Oecologia 152, 583–594. https://doi.org/10.1007/s00442-007-0679-1

Jacobs, D.S., Bastian, A., 2018. High duty cycle echolocation may constrain the evolution of diversity within horseshoe bats (family: Rhinolophidae). Diversity 10. https://doi.org/10.3390/d10030085

Jacobs, D.S., Catto, S., Mutumi, G.L., Finger, N., Webala, P.W., 2017. Testing the Sensory Drive Hypothesis: Geographic variation in echolocation frequencies of Geoffroy's horseshoe bat (Rhinolophidae: *Rhinolophus clivosus*). PLoS One 12. https://doi.org/10.1371/journal.pone.0187769

Jakobsen, L., Brinkløv, S., Surlykke, A., 2013. Intensity and directionality of bat echolocation signals. Front. Physiol. 4 Apr, 1–10. https://doi.org/10.3389/fphys.2013.00089

Jakobsen, L., Surlykke, A., 2010. Vespertilionid bats control the width of their biosonar sound beam dynamically during prey pursuit. Proc. Natl. Acad. Sci. U. S. A. 107, 13930–13935. https://doi.org/10.1073/pnas.1006630107

James, F.C., 1970. Geographic size variation in birds and its relationship to climate. Ecology 51, 365–390. https://doi.org/10.2307/1935374

Jiang, T., Wu, H., Feng, J., 2015. Patterns and causes of geographic variation in bat echolocation pulses. Integr. Zool. 10 (5). 241-256. https://doi.org/10.1111/1749-4877.12129

Jones, G., 1999. Scaling of echolocation call parameters in bats. J. Exp. Biol. 202, 3359–3367.

Jones, G., 1996. Does echolocation constrain the evolution of body size in bats?, in: Symposia of the Zoological Society of London. pp. 111–128.

Jones, G., Gordon, T., Nightingale, J., 1992. Sex and age differences in the echolocation calls of the lesser horseshoe bat, *Rhinolophus hipposideros*. Mammalia 56, 189–194. https://doi.org/10.1515/mamm-1992-0202

Jones, G., Holderied, M.W., 2007. Bat echolocation calls: Adaptation and convergent evolution. Proc. R. Soc. B Biol. Sci. https://doi.org/10.1098/rspb.2006.0200

Jones, G., Jacobs, D.S., Kunz, T.H., Wilig, M.R., Racey, P.A., 2009. Carpe noctem: The importance of bats as bioindicators. Endanger. Species Res. https://doi.org/10.3354/esr00182

Jones, G., Morton, M., Hughes, P.M., Budden, R.M., 1993. Echolocation, flight morphology and foraging strategies of some West African hipposiderid bats. J. Zool. 230, 385–400. https://doi.org/10.1111/j.1469-7998.1993.tb02691.x

Jones, G., Siemers, B.M., 2011. The communicative potential of bat echolocation pulses. J.

Comp. Physiol. A Neuroethol. Sensory, Neural, Behav. Physiol. https://doi.org/10.1007/s00359-010-0565-x

Kalka, M., Kalko, E.K.V., 2006. Gleaning bats as underestimated predators of herbivorous insects: Diet of *Micronycteris microtis* (Phyllostomidae) in Panama. J. Trop. Ecol. 22, 1–10. https://doi.org/10.1017/S0266467405002920

Kalko, E.K.V., Schnitzler, H.U., 1993. Plasticity in echolocation signals of European pipistrelle bats in search flight: implications for habitat use and prey detection. Behav. Ecol. Sociobiol. 33, 415–428. https://doi.org/10.1007/BF00170257

Kearney, M.R., Simpson, S.J., Raubenheimer, D., Kooijman, S.A.L.M., 2013. Balancing heat, water and nutrients under environmental change: A thermodynamic niche framework. Funct. Ecol. 27, 950–966. https://doi.org/10.1111/1365-2435.12020

Kerth, G., Weissmann, K., König, B., 2001. Day roost selection in female Bechstein's bats (*Myotis bechsteinii*): A field experiment to determine the influence of roost temperature. Oecologia 126, 1–9. https://doi.org/10.1007/s004420000489

Klüg-Baerwald, B.J., Gower, L.E., Lausen, C.L., Brigham, R.M., 2016. Environmental correlates and energetics of winter flight by bats in Southern Alberta, Canada. Can. J. Zool. 94, 829–836. https://doi.org/10.1139/cjz-2016-0055

Kluger, M.J., Heath, J.E., 1970. Vasomotion in the bat wing: A thermoregulatory response to internal heating. Comp. Biochem. Physiol. 32, 219–226. https://doi.org/10.1016/0010-406X(70)90935-7

Knörnschild, M., Jung, K., Nagy, M., Metz, M., Kalko, E., 2012. Bat echolocation calls facilitate social communication. Proc. R. Soc. B Biol. Sci. 279, 4827–4835. https://doi.org/10.1098/rspb.2012.1995

Krishna, A., Bhatnagar, K.P., 2011. Hormones and reproductive cycles in bats, in: Hormones and Reproduction of Vertebrates - Volume 5. pp. 241–289. https://doi.org/10.1016/B978-0-12-374928-4.10012-4

Kunz, T.H., 1974. Feeding ecology of a temperate insectivorous bat (*Myotis velifer*). Ecology 55, 693–711. https://doi.org/10.2307/1934408

Kunz, T.H., Fenton, M.B., 2003. Bat Ecology. University of Chicago Press, Chicago.

Lancaster, W.C., Thomson, S.C., Speakman, J.R., 1997. Wing temperature in flying bats measured by infrared thermography. J. Therm. Biol. 22, 109–116. https://doi.org/10.1016/S0306-4565(96)00039-3

Lawrence, B.D., Simmons, J.A., 1982. Measurements of atmospheric attenuation at ultrasonic frequencies and the significance for echolocation by bats. J. Acoust. Soc. Am. 71, 585–590. https://doi.org/10.1121/1.387529

Lazure, L., Fenton, M.B., 2011. High duty cycle echolocation and prey detection by bats. J. Exp. Biol. 214, 1131–1137. https://doi.org/10.1242/jeb.048967

Lobelia, 2020. Past Climate Explorer [WWW Document]. URL https://era5.lobelia.earth/ (accessed 8.11.20).

Lučan, R.K., Weiser, M., Hanák, V., 2013. Contrasting effects of climate change on the timing of reproduction and reproductive success of a temperate insectivorous bat. J. Zool. 290, 151–159. https://doi.org/10.1111/jzo.12021

Luo, J., Koselj, K., Zsebok, S., Siemers, B.M., Goerlitz, H.R., 2014. Global warming alters sound transmission: Differential impact on the prey detection ability of echolocating bats. J. R. Soc. Interface 11. https://doi.org/10.1098/rsif.2013.0961

Lyman P., C., 1970. Thermoregulation and metabolism in bats, in: Wimsatt, W.A. (Ed.), Biology of Bats. Academic Press, New York, New York, pp. 301–329.

Maher, S.P., Kramer, A.M., Pulliam, J.T., Zokan, M.A., Bowden, S.E., Barton, H.D., Magori, K., Drake, J.M., 2012. Spread of white-nose syndrome on a network regulated by geography and climate. Nat. Commun. 3. https://doi.org/10.1038/ncomms2301

Maluleke, T., Jacobs, D.S., Winker, H., 2017. Environmental correlates of geographic divergence in a phenotypic trait: A case study using bat echolocation. Ecol. Evol. 7, 7347–7361. https://doi.org/10.1002/ece3.3251

Matsuta, N., Hiryu, S., Fujioka, E., Yamada, Y., Riquimaroux, H., Watanabe, Y., 2013. Adaptive beam-width control of echolocation sounds by CF-FM bats, *Rhinolophus ferrumequinum nippon,* during prey-capture flight. J. Exp. Biol. 216, 1210–1218. https://doi.org/10.1242/jeb.081398

McNab, B.K., 1969. The economics of temperature regulation in neutropical bats. Comp. Biochem. Physiol. 31, 227–268. https://doi.org/10.1016/0010-406X(69)91651-X

Mead, R.A., 1993. Embryonic diapause in vertebrates. J. Exp. Zool. 266, 629–641. https://doi.org/10.1002/jez.1402660611

Meiri, S., Dayan, T., 2003. On the validity of Bergmann's rule. J. Biogeogr. 30, 331–351. https://doi.org/10.1046/j.1365-2699.2003.00837.x

Monadjem, A., Taylor, P.J., Cotterill, F.P.D., Schoeman, M.C., 2011. Bats of Southern and Central Africa: A Biogeographic and Taxonomic Synthesis, African Zoology. WITS University Press, Johannesburg. https://doi.org/10.1080/15627020.2011.11407657

Mucina, L., Geldenhuys, C.J., Rutherford, M.C., Powrie, L.W., Lötter, M.C., von Maltitz, G.P., Euston-Brown, D.I.W., Matthews, W.S., Dobson, L., McKenzie, B., 2006a. Afrotemperate, Subtropical and Azonal Forests, in: South African Biodiversity Institute (Ed.), The

Vegetation of South Africa, Lesotho and Swaziland. Strelitzia 19. Pretoria, pp. 584–615.

Mucina, L., Jürgens, N., le Roux, A., Rutherford, M.C., Schmiedel, U., Esler, K.J., Powrie, L.W., Desmet, P.G., Milton, S.J., 2006b. Succulent Karoo Biome, in: The Vegetation of South Africa, Lesotho and Swaziland. Strelitzia 19. South African Biodiversity Institute, Pretoria, pp. 220–299.

Mutumi, G.L., Jacobs, D.S., Winker, H., 2016. Sensory drive mediated by climatic gradients partially explains divergence in acoustic signals in two horseshoe bat species, R*hinolophus swinnyi* and *Rhinolophus simulator*. PLoS One 11. https://doi.org/10.1371/journal.pone.0148053

Neuweiler, G., 1990. Auditory adaptations for prey capture in echolocating bats. Physiol. Rev. https://doi.org/10.1152/physrev.1990.70.3.615

Neuweiler, G., Metzner, W., Heilmann, U., Rübsamen, R., Eckrich, M., Costa, H.H., 1987. Foraging behaviour and echolocation in the rufous horseshoe bat (*Rhinolophus rouxi*) of Sri Lanka. Behav. Ecol. Sociobiol. 20, 53–67. https://doi.org/10.1007/BF00292166

Norberg, U.M., 1981. Allometry of bat wings and legs and comparison with birds wings. Philos. Trans. R. Soc. London. B, Biol. Sci. 292, 359–398. https://doi.org/10.1098/rstb.1981.0034

Norberg, U.M., Rayner, J.M. V., 1987. Ecological morphology and flight in bats (Mammalia; Chiroptera): wing adaptations, flight performance, foraging strategy and echolocation. Philos. Trans. R. Soc. London. B, Biol. Sci. 316, 335–427. https://doi.org/10.1098/rstb.1987.0030

O'Shea, T.J., Johnston, J.J., 2017. Environmental contaminants and bats: Investigating exposure and effects, in: Kunz TH, Parsons S (Eds) Ecological and behavioral methods for the study of bats. Johns Hopkins University Press, Baltimore, MD, pp. 500–528.

Odendaal, L.J., Jacobs, D.S., 2011. Morphological correlates of echolocation frequency in the endemic Cape horseshoe bat, *Rhinolophus capensis* (Chiroptera: Rhinolophidae). J. Comp. Physiol. A Neuroethol. Sensory, Neural, Behav. Physiol. 197, 435–446. https://doi.org/10.1007/s00359-010-0601-x

Odendaal, L.J., Jacobs, D.S., Bishop, J.M., 2014. Sensory trait variation in an echolocating bat suggests roles for both selection and plasticity. BMC Evol. Biol. 14. https://doi.org/10.1186/1471-2148-14-60

Pettorelli, N., Vik, J.O., Mysterud, A., Gaillard, J.M., Tucker, C.J., Stenseth, N.C., 2005. Using the satellite-derived NDVI to assess ecological responses to environmental change. Trends Ecol. Evol. 20, 503–510. https://doi.org/10.1016/j.tree.2005.05.011

Racey, P.A., 1973. Environmental factors affecting the length of gestation in heterothermic bats. J. Reprod. Fertil. Suppl. 19, 175–189.

Racey, P.A., 1969. Diagnosis of pregnancy and experimental extension of gestation in the pipistrelle bat, *Pipistrellus pipistrellus*. J. Reprod. Fertil. 19, 465–474. https://doi.org/10.1530/jrf.0.0190465

Rebelo, A.G., Boucher, C., Helme, N., Mucina, L., Rutherford, M.C., 2006. Fynbos Biome, in: The Vegetation of South Africa, Lesotho and Swaziland. Strelitzia 19. South African Biodiversity Institute, Pretoria, pp. 52–219.

Reeder, W.G., Cowles, R.B., 1951.Aspects of thermoregulation in bats. J. Mammology 71 (4), 3–6. https://doi.org/10.1644/869.1.Key

Reichard, J.D., Fellows, S.R., Frank, A.J., Kunz, T.H., 2010. Thermoregulation during flight: Body temperature and sensible heat transfer in free-ranging Brazilian free-tailed bats (*Tadarida brasiliensis*). Physiol. Biochem. Zool. 83, 885–897.

https://doi.org/10.1086/657253

Rhodes, M.P., 1995. Wing morphology and flight behaviour of the golden-tipped bat, *Phoniscus papuensis* (*dobson*) (chiroptera: Vespertilionidae). Aust. J. Zool. 43, 657–663. https://doi.org/10.1071/ZO9950657

Robinson, M.F., 1996. A relationship betwen echolocation calls and noseleaf widths in bats of the genera rhinolophus and hipposideros. J. Zool. 239, 389–393. https://doi.org/10.1111/j.1469-7998.1996.tb05459.x

Rummel, A.D., Swartz, S.M., Marsh, R.L., 2019. Warm bodies, cool wings: Regional heterothermy in flying bats. Biol. Lett. 15. https://doi.org/10.1098/rsbl.2019.0530

Rutherford, M.C., Mucina, L., Powrie, L.W., 2006. Biomes and Bioregions of Southern Africa, in: The Vegetation of South Africa, Lesotho and Swaziland. Strelitzia 19. South African Biodiversity Institute, Pretoria, pp. 30–51. https://doi.org/10.1289/ehp.7863

Rydell, J., 1995. Signal strength, timing, and self-deafening: The evolution of echolocation in bats. Paleobiology 21, 229–242. https://doi.org/10.1017/S0094837300013221

Rydell, J., Jones, G., Waters, D., 1995. Echolocating bats and hearing moths: Who are the winners? Oikos 73, 419. https://doi.org/10.2307/3545970

Scheiter, S., Higgins, S.I., 2009. Impacts of climate change on the vegetation of Africa: An adaptive dynamic vegetation modelling approach. Glob. Chang. Biol. 15, 2224–2246. https://doi.org/10.1111/j.1365-2486.2008.01838.x

Schnitzler, H.U., 1990. Information in sonar echoes of fluttering insects available for echolocating bats. J. Acoust. Soc. Am. 87, 882–896. https://doi.org/10.1121/1.398898

Schnitzler, H.U., 1968. Die ultraschall-ortungslaute der hufeisen-fledermäuse (chiroptera-rhinolophidae) in verschiedenen orientierungssituationen. Z. Vgl. Physiol. 57, 376–408.

https://doi.org/10.1007/BF00303062

Schnitzler, H.U., Denzinger, A., 2011. Auditory fovea and Doppler shift compensation: Adaptations for flutter detection in echolocating bats using CF-FM signals. J. Comp. Physiol. A Neuroethol. Sensory, Neural, Behav. Physiol. https://doi.org/10.1007/s00359-010-0569-6

Schnitzler, H.U., Kalko, E.K.V., 2001. Echolocation by insect-eating bats. Bioscience 51, 557–569. https://doi.org/10.1641/0006-3568(2001)051[0557:EBIEB]2.0.CO;2

Schnitzler, H.U., Moss, C.F., Denzinger, A., 2003. From spatial orientation to food acquisition in echolocating bats. Trends Ecol. Evol. 18, 386–394. https://doi.org/10.1016/S0169-5347(03)00185-X

Schuchmann, M., Siemers, B.M., 2010. Variability in echolocation call intensity in a community of horseshoe bats: A role for resource partitioning or communication? PLoS One 5, 1–9. https://doi.org/10.1371/journal.pone.0012842

Schuller, G., 1974. The role of overlap of echo with outgoing echolocation sound in the bat *Rhinolophus ferrumequinum*. Naturwissenschaften 61, 171–172. https://doi.org/10.1007/BF00602598

Schuller, G., Pollak, G., 1979. Disproportionate frequency representation in the inferior colliculus of doppler-compensating greater horseshoe bats: Evidence for an acoustic fovea. J. Comp. Physiol. https://doi.org/10.1007/BF00617731

Senawi, J., Kingston, T., 2019. Clutter negotiating ability in an ensemble of forest interior bats is driven by body mass. J. Exp. Biol. 22, 1–12. https://doi.org/10.1242/jeb.203950

Sherwin, H.A., Montgomery, W.I., Lundy, M.G., 2013. The impact and implications of climate change for bats. Mamm. Rev. 43, 171–182. https://doi.org/10.1111/j.1365-

2907.2012.00214.x

Simmons, J.A., 2014. Observing the Invisible : Using microphone arrays to study bat echolocation. Acoust. Today. 16-23.

Stawski, C., Geiser, F., 2010. Seasonality of torpor patterns and physiological variables of a free-ranging subtropical bat. J. Exp. Biol. 213, 393–399. https://doi.org/10.1242/jeb.038224

Stilz, W.-P., Schnitzler, H.-U., 2012. Estimation of the acoustic range of bat echolocation for extended targets. J. Acoust. Soc. Am. 132, 1765–1775. https://doi.org/10.1121/1.4733537

Stoffberg, S., 2008. *Rhinolophus capensis* (Chiroptera: Rhinolophidae). Mamm. Species. https://doi.org/10.1644/810.1

Stoffberg, S., 2007. Molecular phylogenetics and the evolution of high-frequency echolocation in horseshoe bats (Genus Rhinolophus). University of Cape Town.

Stoffberg, S., Jacobs, D.S., Matthee, C.A., 2011. The divergence of echolocation frequency in horseshoe bats: Moth hearing, body size or habitat? J. Mamm. Evol. 18, 117–129. https://doi.org/10.1007/s10914-011-9158-x

Strother, G.K., Mogus, M., 1970. Acoustical beam patterns for bats: Some theoretical considerations. J. Acoust. Soc. Am. https://doi.org/10.1121/1.1912304

Suga, N., Jen, P.H.S., 1975. Peripheral control of acoustic signals in the auditory system of echolocating bats. J. Exp. Biol. 62, 277–311. https://doi.org/10.1242/jeb.62.2.277

Sun, K., Luo, L., Kimball, R.T., Wei, X., Jin, L., Jiang, T., Li, G., Feng, J., 2013. Geographic Variation in the acoustic traits of greater horseshoe bats: Testing the importance of drift and ecological selection in evolutionary processes. PLoS One 8. https://doi.org/10.1371/journal.pone.0070368

Surlykke, A., Kalko, E.K.V., 2008. Echolocating bats cry out loud to detect their prey. PLoS One

3. https://doi.org/10.1371/journal.pone.0002036

Surlykke, A., Pedersen, S.B., Jakobsen, L., 2009. Echolocating bats emit a highly directional sonar sound beam in the field. Proc. R. Soc. B Biol. Sci. 276, 853–860. https://doi.org/10.1098/rspb.2008.1505

Taylor, P.J., Macdonald, A., Goodman, S.M., Kearney, T., Cotterill, F.P.D., Stoffberg, S., Monadjem, A., Schoeman, M.C., Guyton, J., Naskrecki, P., Richards, L.R., 2018. Integrative taxonomy resolves three new cryptic species of small southern African horseshoe bats (Rhinolophus). Zool. J. Linn. Soc. 184, 1249–1276. https://doi.org/10.1093/zoolinnean/zly024

Taylor, P.J., Stoffberg, S., Monadjem, A., Schoeman, M.C., Bayliss, J., Cotterill, F.P.D., 2012. Four new bat species (*Rhinolophus hildebrandtii complex*) reflect Plio-Pleistocene divergence of dwarfs and giants across an Afromontane archipelago. PLoS One 7, 1-23 https://doi.org/10.1371/journal.pone.0041744

Thomas, S.P., Follette, D.B., Farabaugh, A.T., 1991. Influence of air temperature on ventilation rates and thermoregulation of a flying bat. Am. J. Physiol. - Regul. Integr. Comp. Physiol. 960-968. https://doi.org/10.1152/ajpregu.1991.260.5.r960

Twente, J.W., 1955. Some aspects of habitat selection and other behavior of cavern-dwelling bats. Ecology 36, 706–732. https://doi.org/10.2307/1931308

Urick, R.J., 1983. Principles of underwater sound. 3rd Edition.

Vaughan, N., Jones, G., Harris, S., 1996. Effects of sewage effluent on the activity of bats (Chiroptera: Vespertilionidae) foraging along rivers. Biol. Conserv. 78, 337–343. https://doi.org/10.1016/S0006-3207(96)00009-2

Vaughan, T.A., 1987. Behavioral thermoregulation in the African yellow-winged bat. J.

Mammal. 68, 376–378. https://doi.org/10.2307/1381476

Vaughan, T.A., 1966. Morphology and flight characteristics of molossid bats. J. Mammal. 47, 249-260. https://doi.org/10.2307/1378121

Vivier, L., Van der Merwe, M., 2007. The incidence of torpor in winter and summer in the Angolan free-tailed bat, *Mops condylurus* (Microchiroptera: Molossidae), in a subtropical environment, Mpumulanga, South Africa. African Zool. 42, 50–58. https://doi.org/10.3377/1562-7020(2007)42[50:TIOTIW]2.0.CO;2

Wang, L.C.H., 1989. Ecological, physiological, and biochemical aspects of torpor in mammals and birds. In: Wang L.C.H. (eds) Animal Adaptation to Cold. Advances in Comparative and Environmental Physiology, vol 4. Springer, Berlin, Heidelberg. https://doi.org/10.1007/978-3-642-74078-7_10

Wang, M., Chen, K., Guo, D., Luo, B., Wang, W., Gao, H., Liu, Y., Feng, J., 2020. Ambient temperature correlates with geographic variation in body size of least horseshoe bats. Curr. Zool. 66, 459–465. https://doi.org/10.1093/cz/zoaa004

Warnecke, M., Chiu, C., Engelberg, J., Moss, C.F., 2015. Active listening in a bat cocktail party: Adaptive echolocation and flight behaviors of big brown bats, *Eptesicus fuscus*, foraging in a cluttered acoustic environment. Brain. Behav. Evol. 86, 6–16. https://doi.org/10.1159/000437346

Wever, E.G., Vernon, J.A., 1961. The protective mechanisms of the bat's ear. Ann. Otol. Rhinol. Laryngol. 70, 5–17. https://doi.org/10.1177/000348946107000101

Widmer, R.J., Stewart, R.H., Young, M.F., Laurinec, J.E., Laine, G.A., Quick, C.M., 2007. Application of local heat induces capillary recruitment in the Pallid bat wing. Am. J. Physiol. - Regul. Integr. Comp. Physiol. 292. https://doi.org/10.1152/ajpregu.00873.2006

Wilson, A.M., Latimer, A.M., Silander, J.A., 2015. Climatic controls on ecosystem resilience: Postfire regeneration in the Cape Floristic Region of South Africa. Proc. Natl. Acad. Sci. U. S. A. 112, 9058–9063. https://doi.org/10.1073/pnas.1416710112

Wu, H., Jiang, T., Huang, X., Feng, J., 2018. Patterns of sexual size dimorphism in horseshoe bats: Testing Rensch's rule and potential causes. Sci. Rep. 8. https://doi.org/10.1038/s41598-018-21077-7

Zechmann, E., 2020. Air Absorption [WWW Document]. MATLAB Cent. File Exch. URL https://www.mathworks.com/matlabcentral/fileexchange/26835-air-absorption (accessed 7.22.20).

Zhang, Y., Lin, A., Ding, J., Yang, X., Jiang, T., Liu, Y., Feng, J., 2019. Performance of Doppler shift compensation in bats varies with species rather than with environmental clutter. Anim. Behav. 158, 109–120. https://doi.org/10.1016/j.anbehav.2019.10.008

APPENDIX

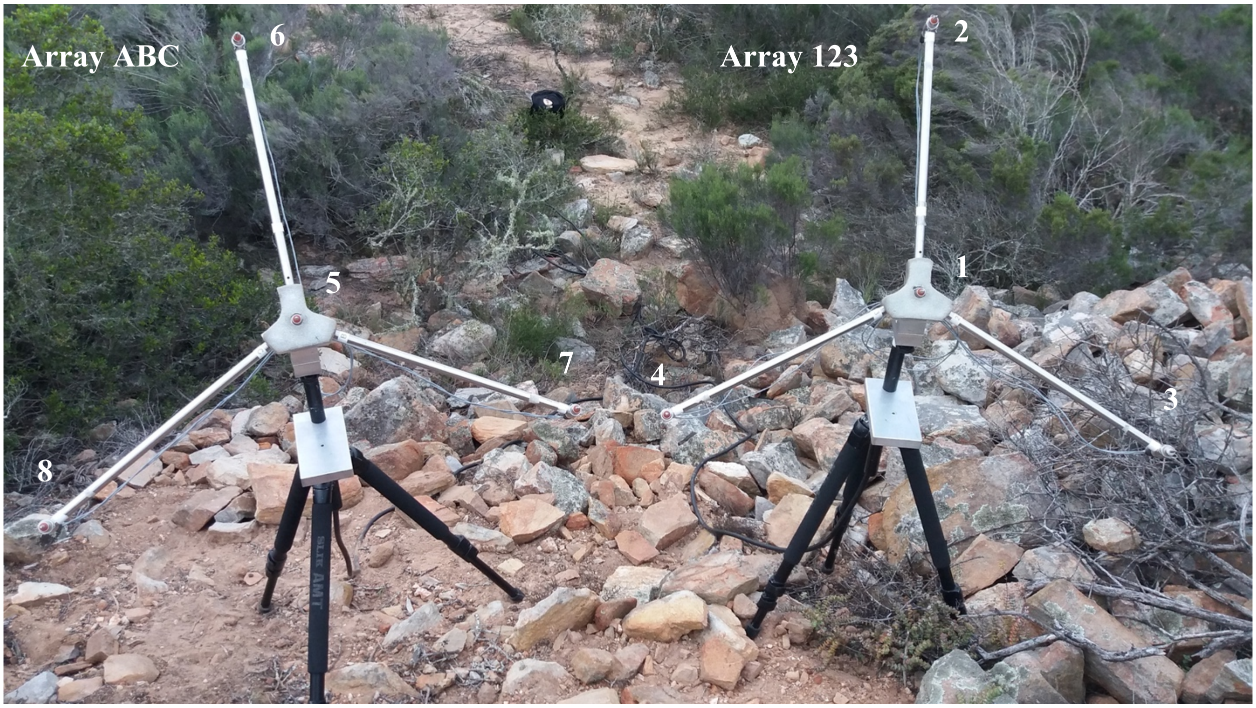

FIGURE A1: The star microphone array system used to record *R. capensis* as it exited the cave to forage. The 8 microphones are labeled one through eight. There were 4 microphones on each of the two arrays, which were labeled Array ABC and Array 123.

TABLE A1: Average source level and average frequency ± mean and standard deviation of echolocation pulses by locality in *R. capensis*

Locality	Average source level (dB) (Mean±SD)	Average frequency (Hz) (Mean +-SD)
Zoutpansklipheuwel	127.31 ± 4.08	78816.02 ± 764.17
Lekkersing	134.27 ± 10.83	73837.81 ± 921.81
De Hoop	128.29 ± 8.49	82606.46 ± 1326.13
Baviaanskloof	125.72 ± 7.55	83338.49 ± 639.98
Table Farm	132.13 ± 3.73	84822.72 ± 1137.68

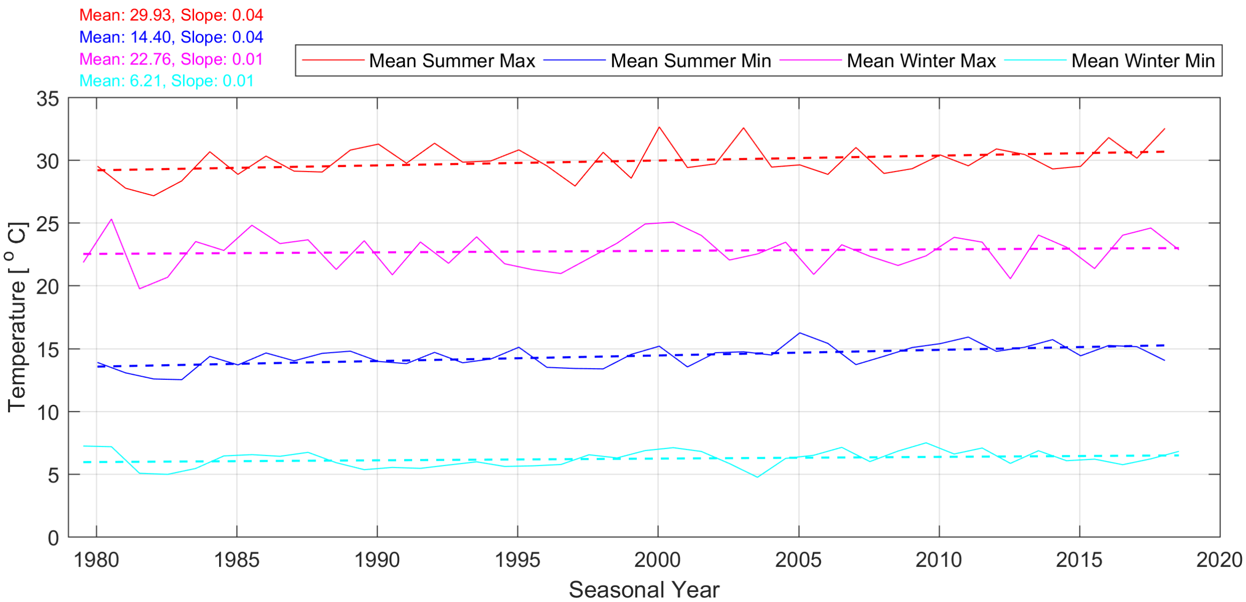

FIGURE A2: Heidehof seasonal climatology. This graph depicts the mean summer maximum temperature, the mean summer minimum temperature, the mean winter maximum temperature, and the mean winter maximum temperature by year. The dash lines represent a 95 percent confidence interval.

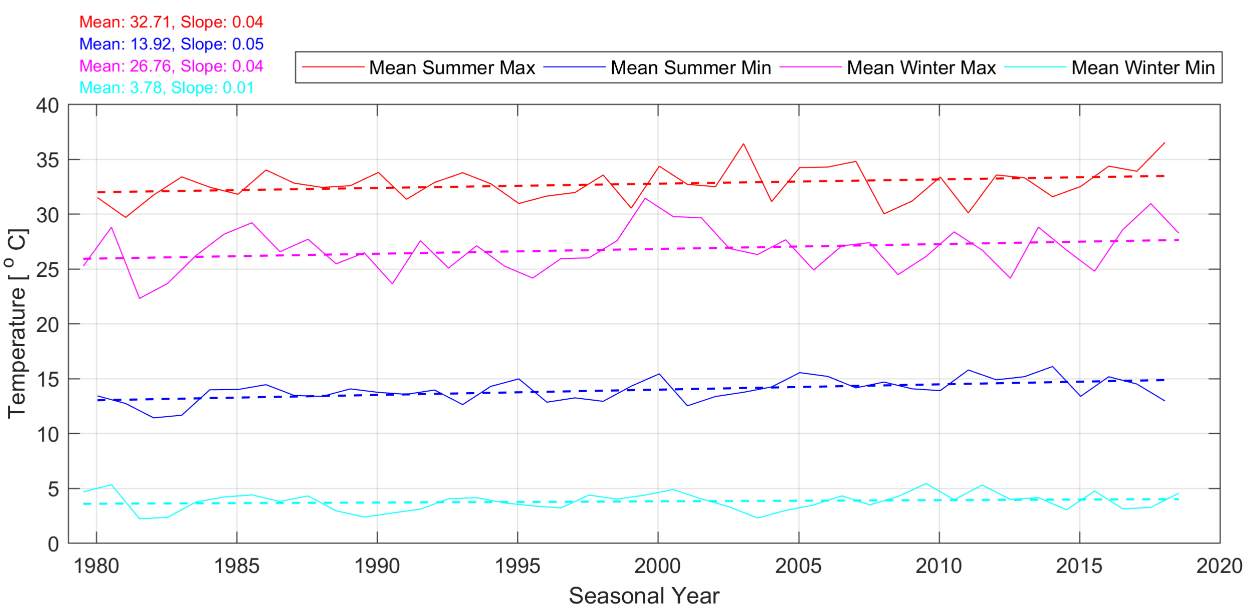

FIGURE A3: De Hoop seasonal climatology. This graph depicts the mean summer maximum temperature, the mean summer minimum temperature, the mean winter maximum temperature, and the mean winter maximum temperature by year. The dash lines represent a 95 percent confidence interval.

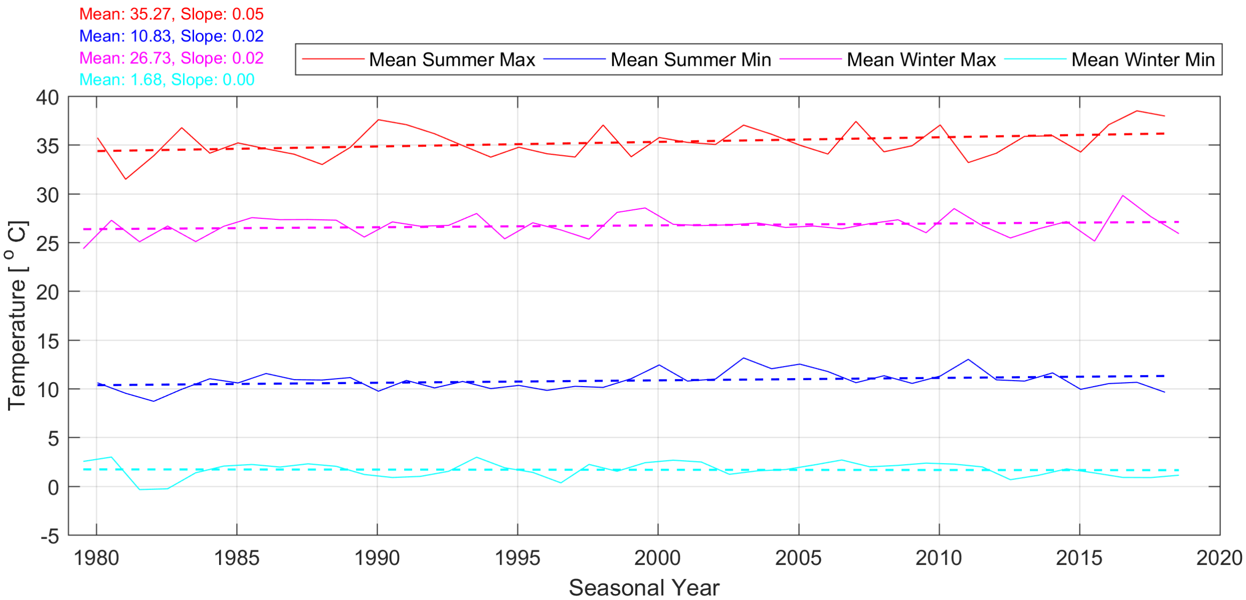

FIGURE A4: Baviaanskloof seasonal climatology. This graph depicts the mean summer maximum temperature, the mean summer minimum temperature, the mean winter maximum temperature, and the mean winter maximum temperature by year. The dash lines represent a 95 percent confidence interval.

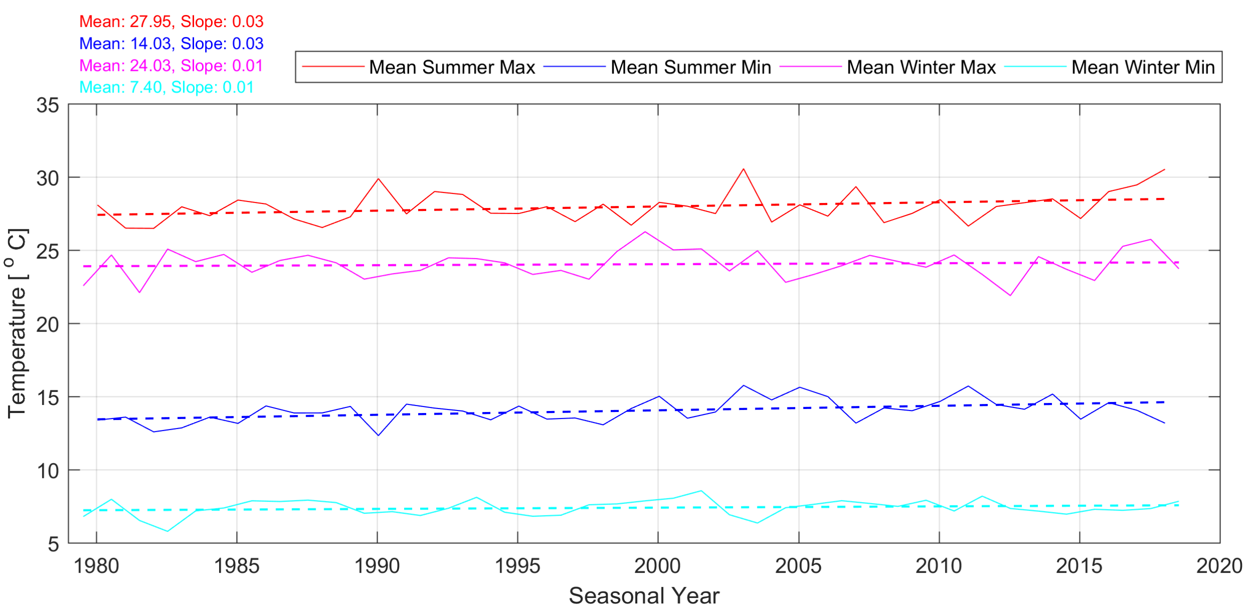

FIGURE A5: Knysna seasonal climatology. This graph depicts the mean summer maximum temperature, the mean summer minimum temperature, the mean winter maximum temperature, and the mean winter maximum temperature by year. The dash lines represent a 95 percent confidence interval.

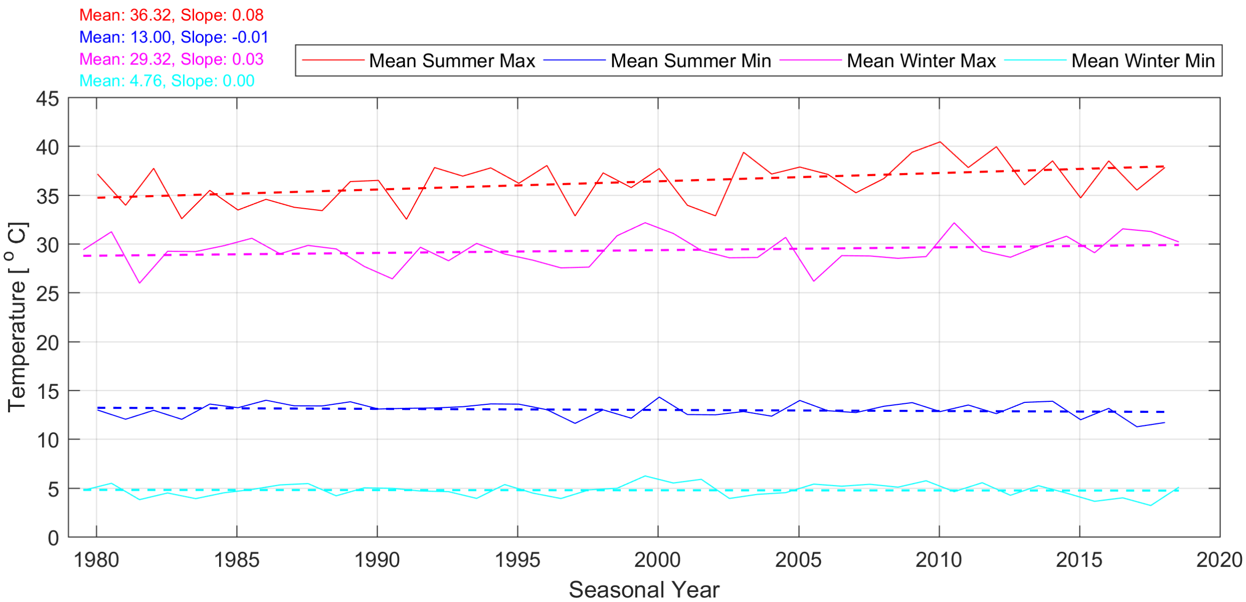

FIGURE A6: Zoutpansklipheuwel seasonal climatology. This graph depicts the mean summer maximum temperature, the mean summer minimum temperature, the mean winter maximum temperature, and the mean winter maximum temperature by year. The dash lines represent a 95 percent confidence interval

.

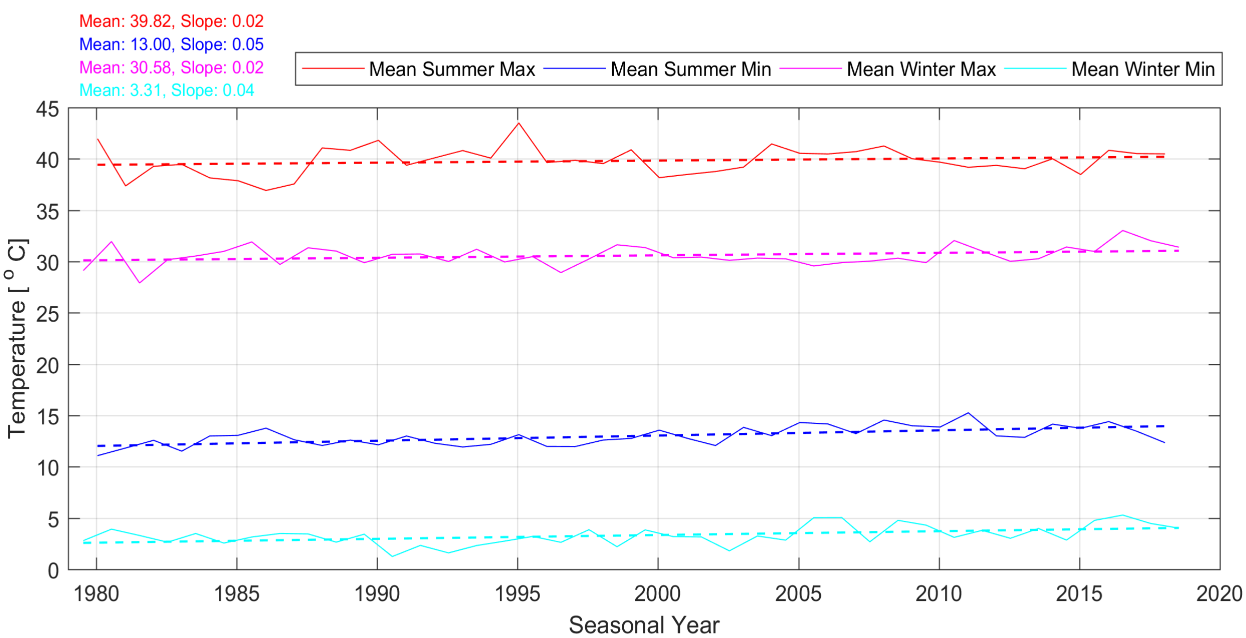

FIGURE A7: Lekkersing seasonal climatology. This graph depicts the mean summer maximum temperature, the mean summer minimum temperature, the mean winter maximum temperature, and the mean winter maximum temperature by year. The dash lines represent a 95 percent confidence interval.

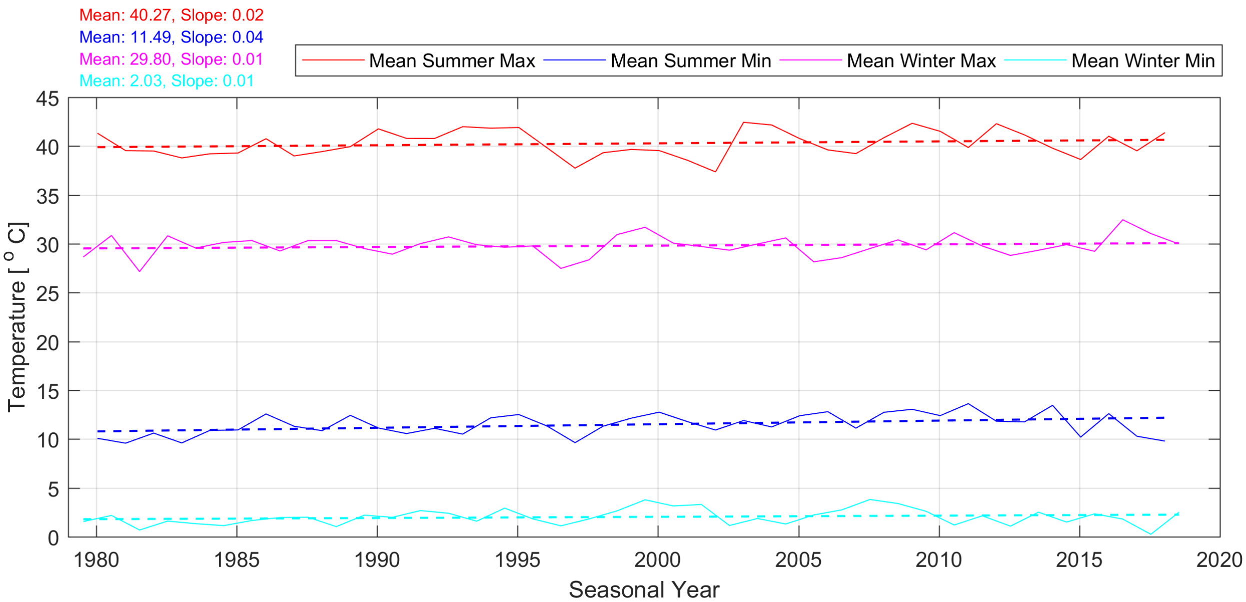

FIGURE A8: Steenkampskraal seasonal climatology. This graph depicts the mean summer maximum temperature, the mean summer minimum temperature, the mean winter maximum temperature, and the mean winter maximum temperature by year. The dash lines represent a 95 percent confidence interval.

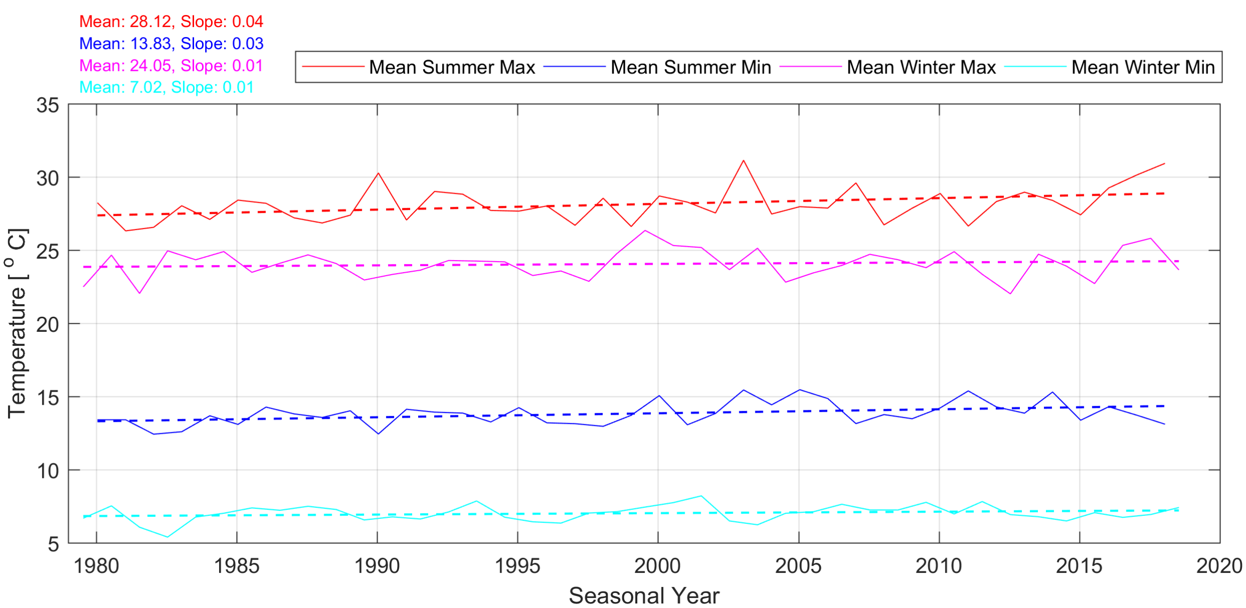

FIGURE A9: Sleepy Hollow seasonal climatology. This graph depicts the mean summer maximum temperature, the mean summer minimum temperature, the mean winter maximum temperature, and the mean winter maximum temperature by year. The dash lines represent a 95 percent confidence interval.

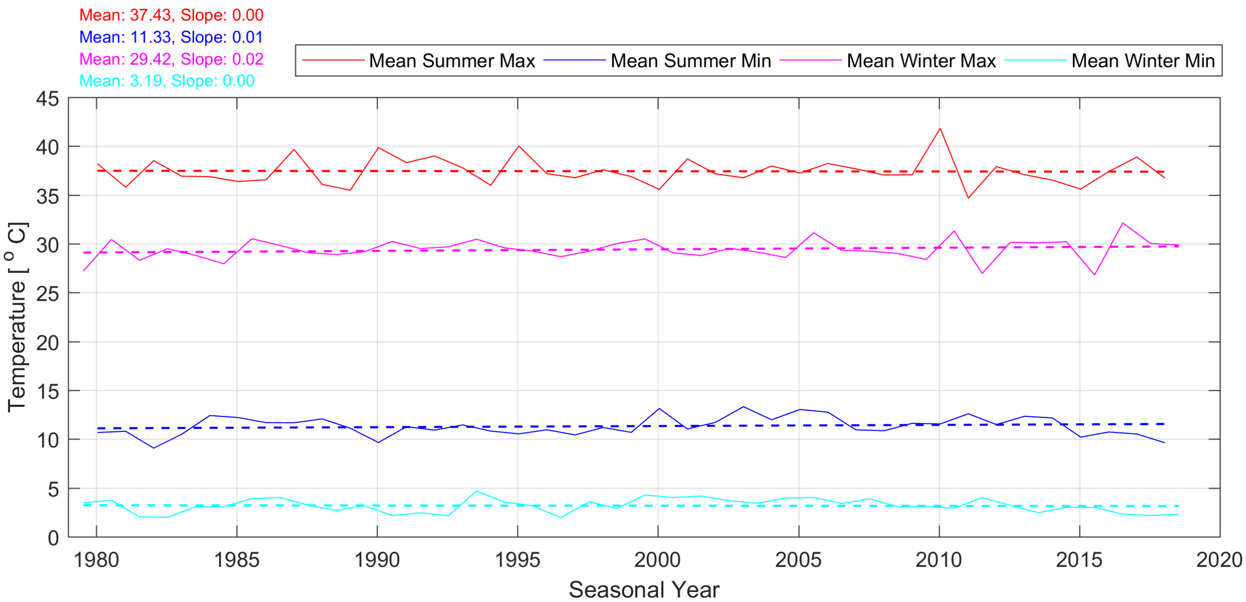

FIGURE A10: Table Farm seasonal climatology. This graph depicts the mean summer maximum temperature, the mean summer minimum temperature, the mean winter maximum temperature, and the mean winter maximum temperature by year. The dash lines represent a 95 percent confidence interval.

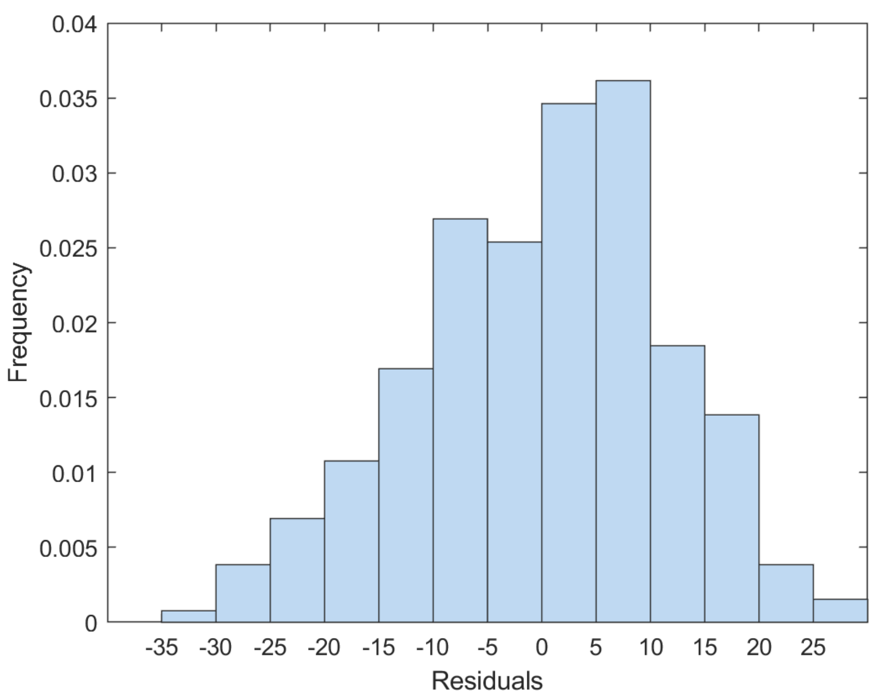

FIGURE A11: Histogram showing the wing area residual of *R. capensis*. The graph depicts a normal distribution.

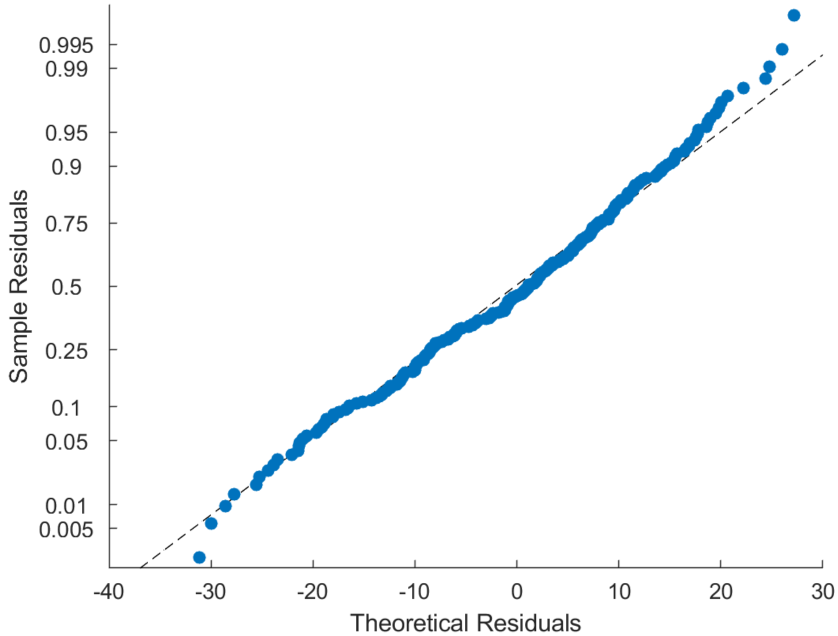

FIGURE A12: Wing area residuals plot showing the theoretical and sample values for wing area in *R. capensis*

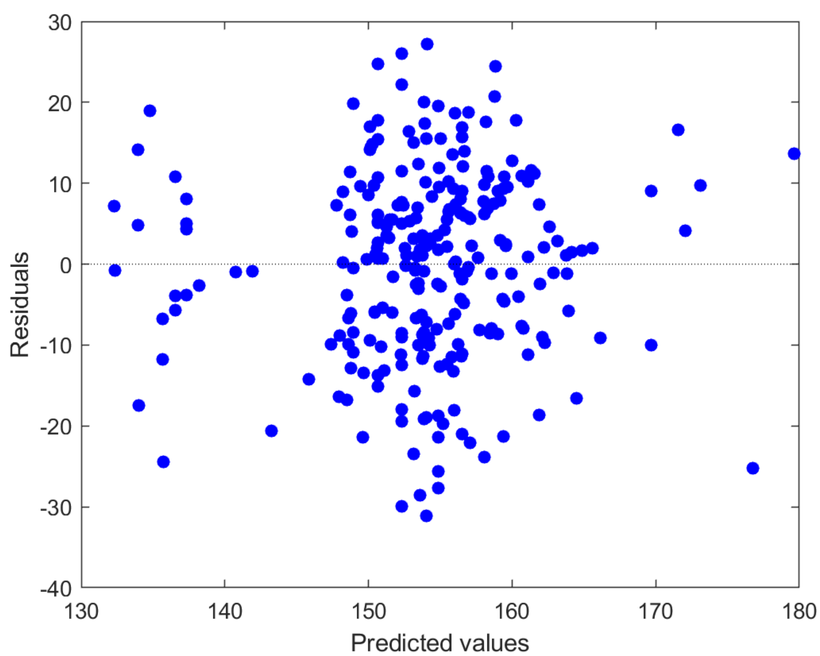

FIGURE A13: Wing area residuals scatterplot showing heteroskedasticity between the predicted values and residual values

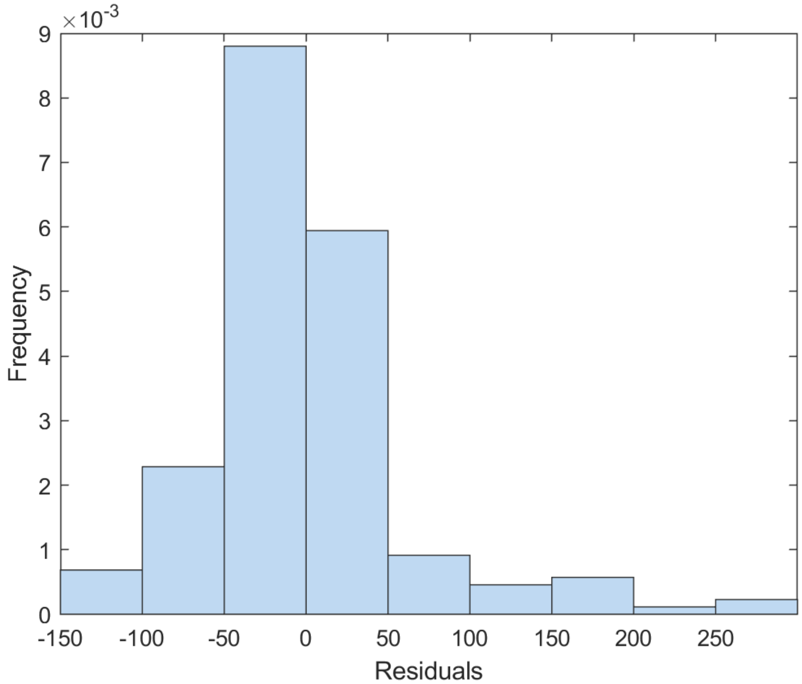

FIGURE A14: Prey detection volume (target strength -65 dB) residual scatterplot of *R. capensis*. This graph depicts a non-normal distribution

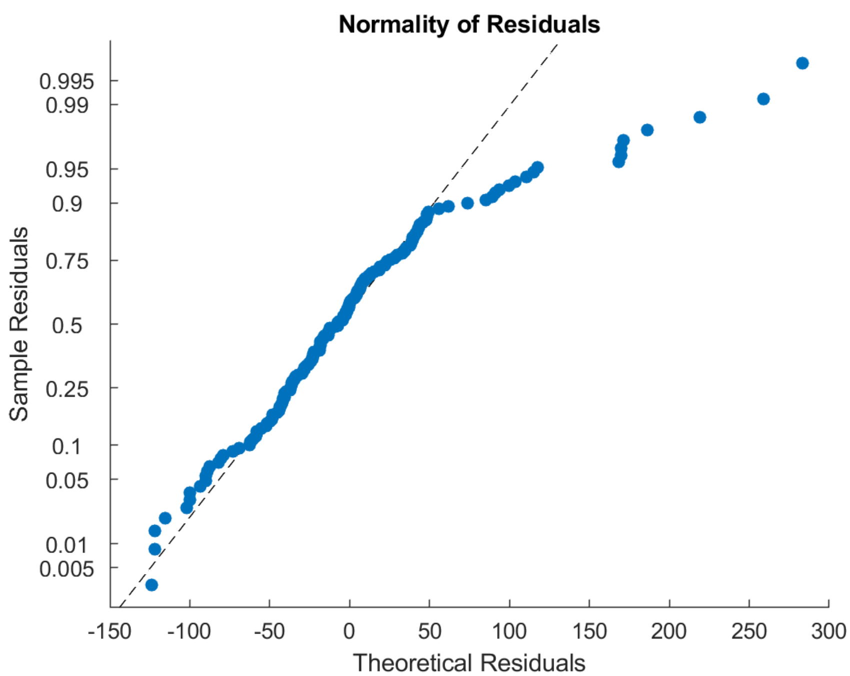

FIGURE A15: Prey detection volume (target strength -65 dB) residuals plot showing theoretical and sample values in *R. capensis*

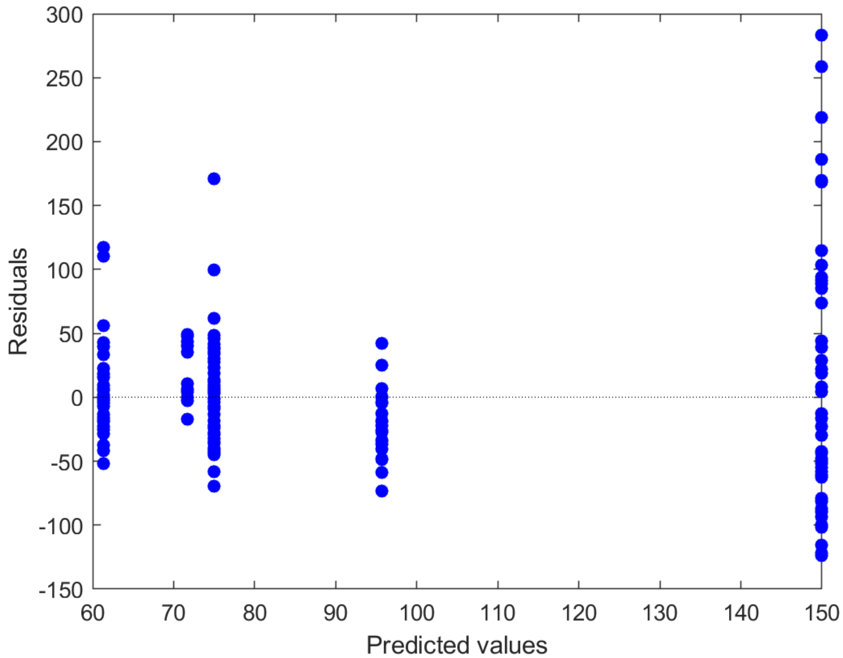

FIGURE A16: Prey detection volume (target strength -65 dB) residual scatterplot showing heteroskedasticity between the predicted values and residual values